

AD-A143 748

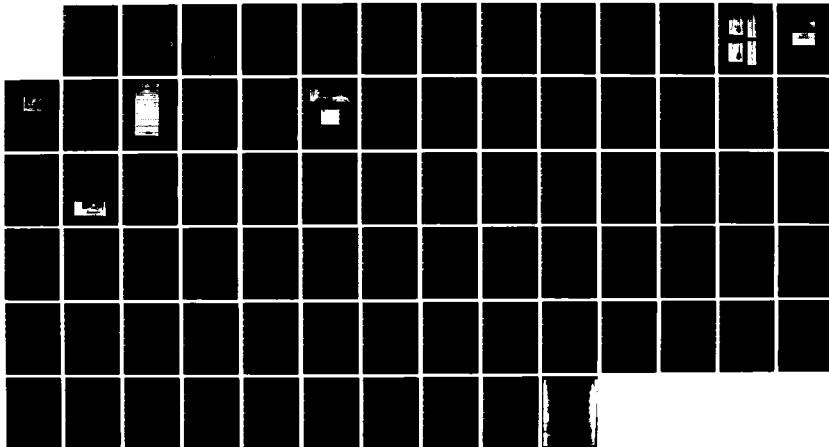
HIGH-CURRENT BETATRON PHASE I(U) MAXEELL LABS INC SAN  
DIEGO CA G BARRAK ET AL. 16 APR 82 MLR-1259  
SBI-AD-E001 397 N00014-80-C-0914

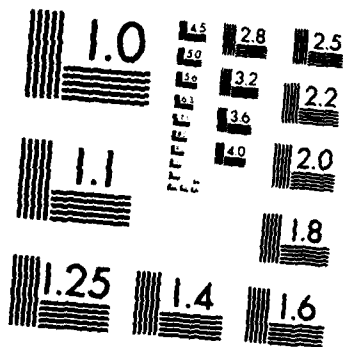
1/1

UNCLASSIFIED

F/G 20/7

NL





MICROCOPY RESOLUTION TEST CHART  
NATIONAL BUREAU OF STANDARDS-1963-A

AD-E001397

①



MLR-1259  
16 APRIL 1982

# FINAL REPORT HIGH-CURRENT BETATRON, PHASE I

COVERING THE PERIOD:

22 SEPTEMBER 1980 -- 15 FEBRUARY 1982

CONTRACT NUMBER:  
N00014-80-C-0914

DTIC  
ELECTE  
JUL 30 1984  
S D  
B

Submitted To:

DEFENSE ADVANCED RESEARCH PROJECTS AGENCY  
1400 WILSON BOULEVARD  
ARLINGTON VA 22209

DISTRIBUTION STATEMENT A  
Approved for public release  
Distribution Unlimited

Prepared By:

MAXWELL LABORATORIES, INC.  
8835 BALBOA AVENUE  
SAN DIEGO CA 92123

AD-A143 748

DTIC FILE COPY

84 07 27 079

AD-A143 7-18

TABLE OF CONTENTS

<u>SECTION</u>	<u>TITLE</u>	<u>PAGE</u>
1-1	INTRODUCTION.....	1-1
1-2	STATEMENT OF WORK (MLR-402-1).....	1-1
1-2.1	Statement of Work (November 1980- June 15, 1981).....	1-1
1-2.2	Statement of Work (June 15- December 31, 1981).....	1-2
1-3	SUMMARY OF RESULTS FOR THE PERIOD JUNE 15-DECEMBER 15, 1981.....	1-4
1-4	EXPERIMENTAL PROGRESS.....	1-4
1-5	INDUCTIVE CHARGING IN A PASSIVE MIRROR.....	1-5
1-6	LIFETIME OF ELECTRONS.....	1-10
1-7	FOUR MIRROR EXPERIMENT.....	1-10
1-8	DISCUSSION.....	1-15



Accession For	
REFS	COMM ✓
DTIC TAB	<input type="checkbox"/>
Unannounced	<input type="checkbox"/>
Distribution/	
Availability Codes	
Dist	Special
<b>A-1</b>	

## LIST OF FIGURES

<u>NUMBER</u>	<u>TITLE</u>	<u>PAGE</u>
1	Betatron experiment.....	1-3
2	Experimental arrangements of equipment.....	1-6
3	Magnetic field (top trace) and electrostatic oscillation (middle). Sweep: 50 $\mu$ s/div. The bottom trace is the fast picture of the electrostatic oscillation.....	1-7
4	Oscilloscope traces of electrostatic oscillations picked up by the anode of electron injector.....	1-8
5	Electrostatic signals from two mirrors. 50 $\mu$ s/div. Upper: $\theta = 0^\circ$ . Lower: $\theta = 135^\circ$ .....	1-9
6	Oscilloscope traces of electrostatic oscillations for different injection voltages.....	1-11
7	Injection voltage dependence of the electrostatic oscillation.....	1-12
8	Frequency of electrostatic oscillation as a function of injected current.....	1-13
9	Waveforms from toroidal experiment.....	1-14

# CONVERSION FACTORS FOR U.S. CUSTOMARY TO METRIC (SI) UNITS OF MEASUREMENT

To Convert From	To	By
angstrom	Meters (m)	1.000 000 x E -10
atmosphere (normal)	Kilo pascal (kPa)	1.013 25 X E +2
bar	kilo pascal (kPa)	1.000 000 X E +2
barn	meter <sup>2</sup> (m <sup>2</sup> )	1.000 000 X E -28
British thermal unit (thermochemical)	joule (J)	1.054 350 X E +3
cal (thermochemical)/cm <sup>2</sup>	meta joule/m <sup>2</sup> (MJ/m <sup>2</sup> )	4.184 000 X E -2
calorie (thermochemical)	joule (J)	4.184 000
calorie (thermochemical)/g	joule per kilogram (J/kg)*	4.184 000 X E +3
curies	giga becquerel (Gq)†	3.700 000 X E +1
degree Celsius	degree kelvin (K)	$T_K = T_C + 273.15$
degree (angle)	radian (rad)	1.745 329 X E -2
degree Fahrenheit	degree kelvin (K)	$T_K = (T_F + 459.67) / 1.8$
electron volt	joule (J)	1.602 19 X E -19
erg	joule (J)	1.000 000 X E -7
erg/second	watt (W)	1.000 000 X E -7
foot	meter (m)	3.048 000 X E -1
foot-pound-force	joule (J)	1.355 818
gallon (U.S. liquid)	meter <sup>3</sup> (m <sup>3</sup> )	3.785 412 X E -3
inch	meter (m)	2.540 000 X E -2
jerk	joule (J)	1.000 000 X E +9
joule kilogram (J/kg) (radiation dose absorbed)	gray (Gy)*	1.000 000
kilotons	terajoules	4.183
kip (1000 lbf)	newton (N)	4.448 222 X E +3
kip/inch <sup>2</sup> (ksi)	kilo pascal (kPa)	6.894 757 X E +3
ktap	newton-second/m <sup>2</sup> (N-s/m <sup>2</sup> )	1.000 000 X E +2
micron	meter (m)	1.000 000 X E -6
mil	meter (m)	2.540 000 X E -5
mile (international)	meter (m)	1.609 344 X E +3
ounce	kilogram (kg)	2.834 952 X E -2
pound-force (lbf avoirdupois)	newton (N)	4.448 222
pound-force inch	newton-meter (N·m)	1.129 848 X E -1
pound-force/inch	newton/meter (N/m)	1.751 268 X E +2
pound-force/foot <sup>2</sup>	kilo pascal (kPa)	4.788 026 X E -2
pound-force/inch <sup>2</sup> (psi)	kilo pascal (kPa)	6.894 757
pound-mass (lbm avoirdupois)	kilogram (kg)	4.535 924 X E -1
pound-mass-foot <sup>2</sup> (moment of inertia)	kilogram-meter <sup>2</sup> (kg·m <sup>2</sup> )	4.214 011 X E -2
pound-mass/foot <sup>3</sup>	kilogram-meter <sup>3</sup> (kg/m <sup>3</sup> )	1.061 846 X E +1
rad (radiation dose absorbed)‡	gray (Gy)*	1.000 000 X E -2
roentgen§	coulomb/kilogram (C/kg)	2.579 760 X E -4
shake	second (s)	1.000 000 X E -8
slug	kilogram (kg)	1.459 390 X E -1
torr (mm Hg, 0° C)	kilo pascal (kPa)	1.333 22 X E -1

\*The gray (Gy) is the accepted SI unit equivalent to the energy imparted by ionizing radiation to a mass and corresponds to one joule/kilogram.

†The becquerel (Bq) is the SI unit of radioactivity; 1 Bq = 1 event/s.

## HIGH-CURRENT BETATRON, PHASE I

### 1-1 INTRODUCTION

In a conventional Betatron, the current is limited by the method of injection and the constant orbit radius. For example, with an injection energy of 100 keV and an orbit radius of 1 m, the initial magnetic field must be  $\sim 10$  G. The current density is limited by space charge of the beam to  $\sim 100$  mA/cm<sup>2</sup>. We proposed (MLR-402-1, April 28, 1980) to construct a device with a toroidal magnetic field of  $\sim 10^4$  G, in which case the space charge limit for the current density is increased by the factor  $10^6$ . We proposed to inject the electrons to form a beam by an adaptation of the method of inductive charging.

### 1-2 STATEMENT OF WORK (MLP-402-1)

The Statement of Work from proposal MLP-402-1 is reproduced below.

#### 1-2.1 Statement of Work (November 1980-June 15, 1981)

##### Task 1. Construct Torus

A glass torus with a 40 cm major radius and 5 cm minor radius will be constructed, coated with epoxy fiberglass and wound with copper wire.

##### Task 2. Design and Fabricate Coils

Vertical-field, air-core coils will be designed and fabricated.

##### Task 3. Assemble Systems

The systems of the Betatron experiment, including magnetic field coils, power supplies, vacuum system, and injectors, will be assembled.

Task 4. Perform Initial Experiments

Initial experiments on injection trapping and acceleration will be performed. Electron current and energy will be measured.

Task 5. Analyze Stability

Electron orbit and beam stability will be investigated analytically and numerically. Stability analyses will be performed for:

- a. Integer and half integer resonances.
- b. Negative mass instability.
- c. Resistive wall/negative energy wave instabilities.

This work was carried out during the period November 1980-June 15, 1981. The results are described in Appendix A.

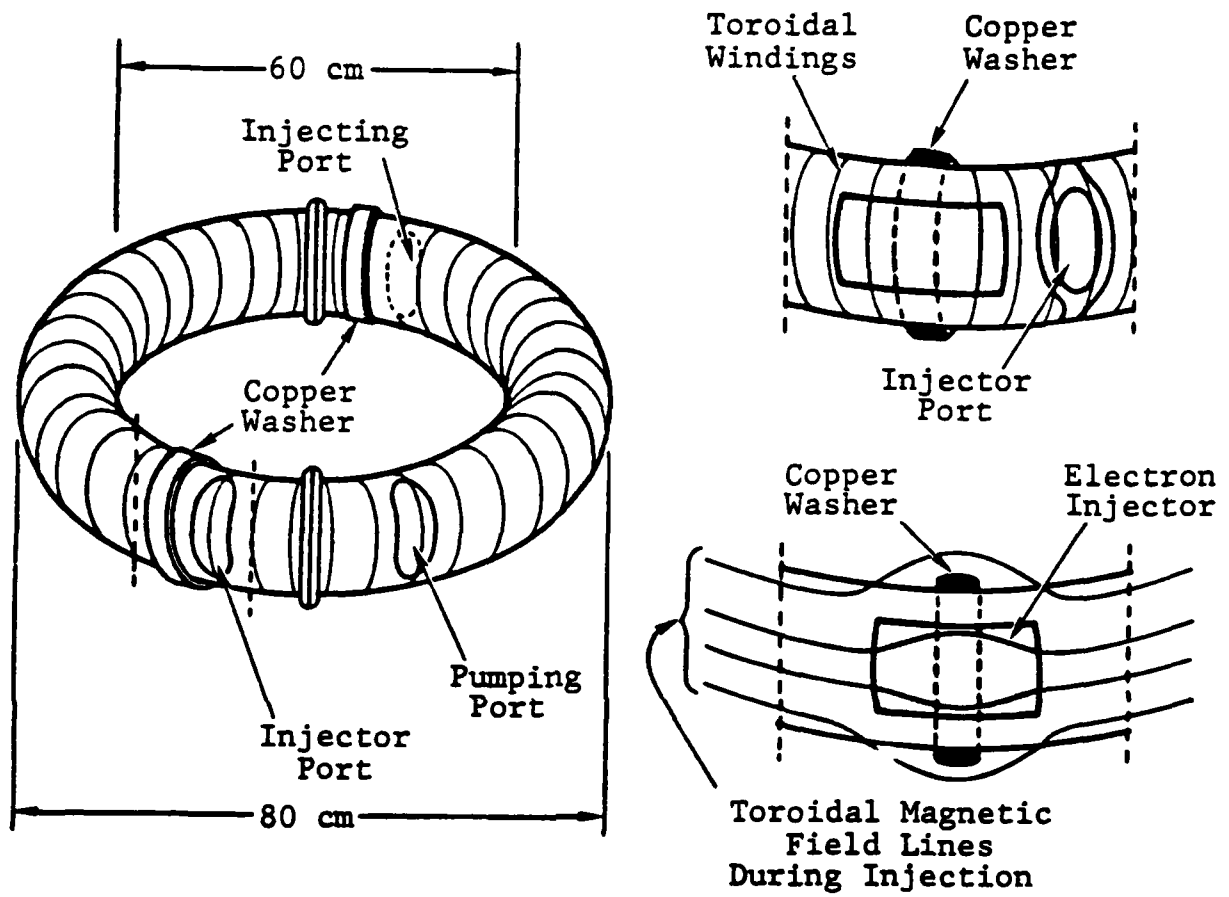
1-2.2 Statement of Work (June 15-December 31, 1981)

Phase I was continued during the period June 15-December 31, 1981. The Statement of Work for this period is reproduced below:

Task 1. Measurement of Injected Charge and Trapping Efficiency

The injected charge can be determined from current traces. The charge trapped can be measured by observing the frequency of diocotron oscillations. The charge will first be trapped in local mirror regions as illustrated in Figure 1. Then, as the diamagnetic current in the copper washer decays, electrons will be ejected along the toroidal field lines. It is important to measure the electron line density before, during and after this process. Parameter studies will be carried out including variations in injector voltage and injector position. We plan to begin with





MLI82-406

Figure 1. Betatron experiment.

one injector and increase the number up to four, as required. The end result of this study should be that a toroidal beam of electrons is trapped and has stable confinement for  $\sim 1$  ms. The mean velocity in the toroidal direction should be zero.

Task 2. Acceleration of the Toroidal Electron Beam  
The Betatron fields will be applied. This involves a peak magnetic field of 1 kG at the location of the beam with a rise time of  $\sim 1$  ms. The toroidal electric field will produce  $\sim 100$  V per revolution. The field index can be varied from 0.2 to 0.8. We will measure the current with a Rogowski coil and monitor the charge per unit length by continuously observing the diocotron frequency. X-ray measurements with scintillators will also be used to monitor the beam. The objective is to document acceleration to a few MeV with a current of the order of 1 kA.

1-3 SUMMARY OF RESULTS FOR THE PERIOD  
JUNE 15-DECEMBER 15, 1981

A local mirror was produced around the electron injectors by weakening the toroidal magnetic field with a closed loop of wires. Electrons were trapped there as well as in a driven mirror. The line density of trapped electrons was proportional to the injection voltage. With the use of four injectors, electrons were captured in four local mirrors along the torus. The current in the loop of wires decayed much faster than the toroidal field resulting in collapse of the local mirror. Electrons were then lost due to toroidal drift as indicated by a delayed burst of X-rays.

1-4 EXPERIMENTAL PROGRESS

Figure 2 shows schematically how the apparatus has been modified. In a previous report, an arrangement was described whereby the mirror field was produced by energizing

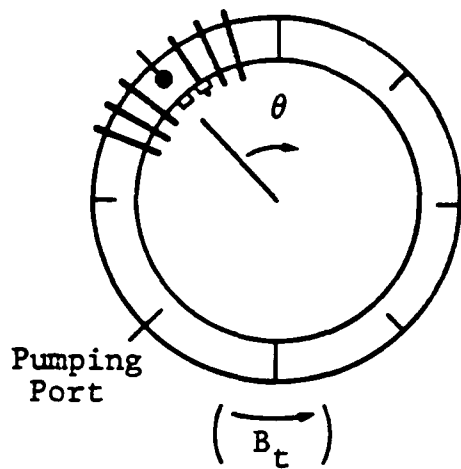
mirror coils with a capacitor bank (Figure 2a). This approach was subsequently abandoned and a passive means was adopted. A pair of stranded cables, 2.5 mm dia, was wound around the injector (Figure 2b). These cables were shorted to form a closed loop. An electric current was induced by the shorted cables by the changing toroidal magnetic field, producing a local mirror.

After electrons were successfully trapped in the mirror formed by the shorted cables, two additional injectors were installed and tested (Figure 2c). The multiple injectors were first fired independently, the A-K gap was adjusted, and some conditions (e.g., heater current) for electron trapping were checked. Electrostatic probes were located in only one mirror. For the remaining two mirrors, the anodes of the electron injectors were used as electrostatic probes. After each injector was tested independently, all three were fired simultaneously and electrons were trapped in three mirrors. The experimental apparatus was disassembled to install additional electrostatic probes and an additional injector. The final configuration involved four injectors, seven shorted cable pairs and seven electrostatic probes (Figure 2d).

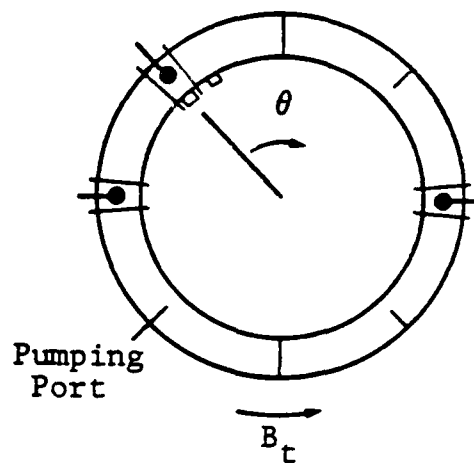
#### 1-5 INDUCTIVE CHARGING IN A PASSIVE MIRROR

A comparison between the driven mirror and the passive mirror is made in Figure 3. In a driven mirror, the electrostatic oscillation lasted longer (Figure 3a). In the passive mirror, the oscillation damped in 150  $\mu$ s (Figure 3b). The oscilloscope traces of the oscillations were, however, quite similar to each other when observed on a fast sweep speed. This suggests that the trapping takes place similarly in both cases.

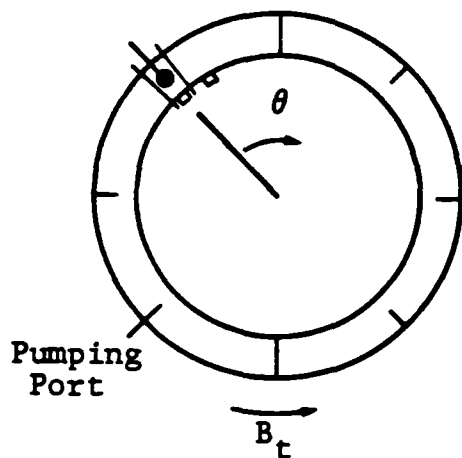
Figure 4 shows the electrostatic oscillations detected by anodes when three injectors were used. Simultaneous trapping was observed as in Figure 5. The frequencies of the oscillations in the three cells were not identical but were nearly the same.



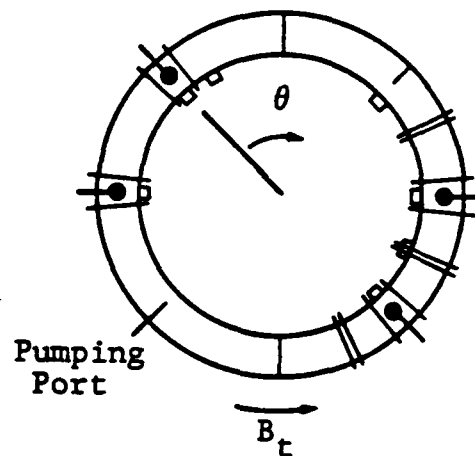
(a) Driven mirror coils.



(c) Three injectors and mirrors.



(b) Passive mirror.

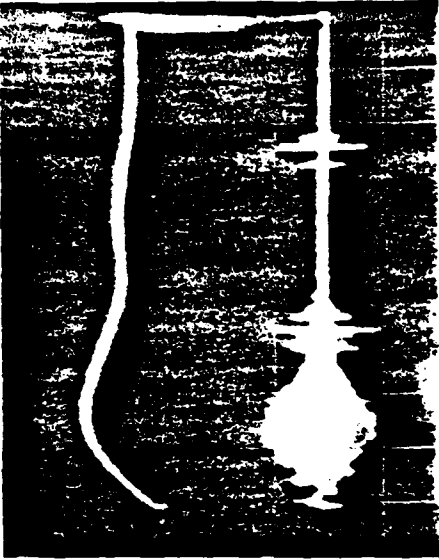


(d) Present state.

- Injector
- Closed Loop
- ⊓ Electrostatic Probe

MLI82-407

Figure 2. Experimental arrangements of equipment.

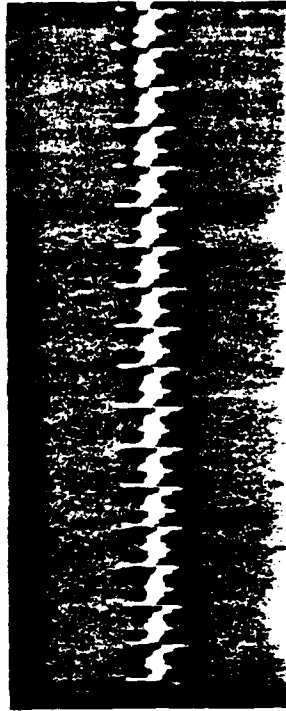


0.5  $\mu$ s



@ 180  $\mu$ s

(a) Driven mirror.

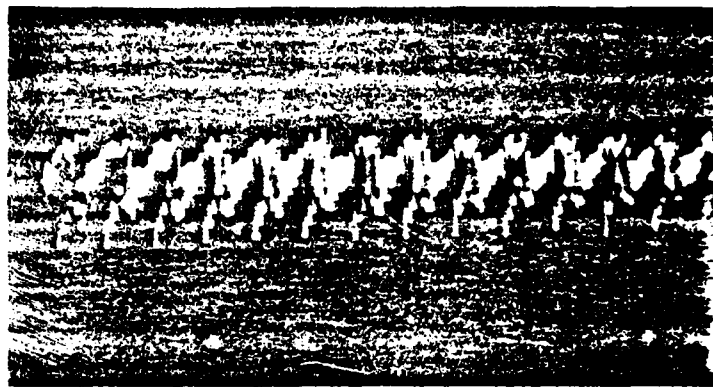


@ 100  $\mu$ s

(b) Passive mirror.

Figure 3. Magnetic field (top trace) and electrostatic oscillation (middle). Sweep: 50  $\mu$ s/div. The bottom trace is the fast picture of the electrostatic oscillation.

ML182-408



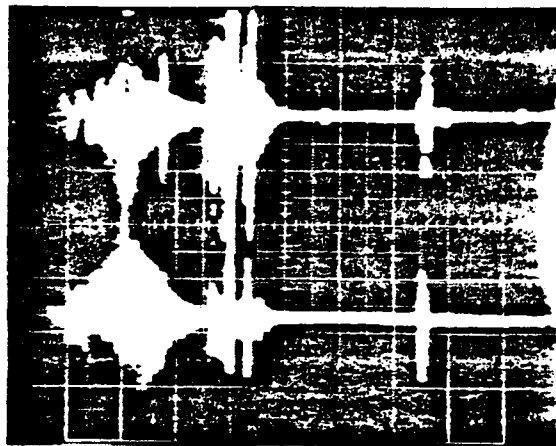
(a)  $\theta = 135^\circ$ .



(b)  $\theta = 315^\circ$ .

ML182-409

Figure 4. Oscilloscope traces of electrostatic oscillations picked up by the anode of electron injector.



Noise

MLI82-410

Figure 5. Electrostatic signals from two mirrors. 50  $\mu$ s/div.  
Upper:  $\theta = 0^\circ$ . Lower:  $\theta = 135^\circ$ .

The dependence of trapping on experimental parameters was studied. Figure 6 shows oscilloscope traces of electrostatic oscillations when changing the injection voltage. All the other parameters were fixed. The frequency is proportional to the injection voltage (Figure 7) in agreement with theory.

The frequency is plotted as a function of injection current in Figure 8. It is noted that the frequency is weakly dependent on the injection current: the frequency variation is within 10 percent for the total injection current of 0.4-2.0 A. The trapping was sensitive to the injection timing, as studied on the collective focusing ion accelerator.

#### 1-6 LIFETIME OF ELECTRONS

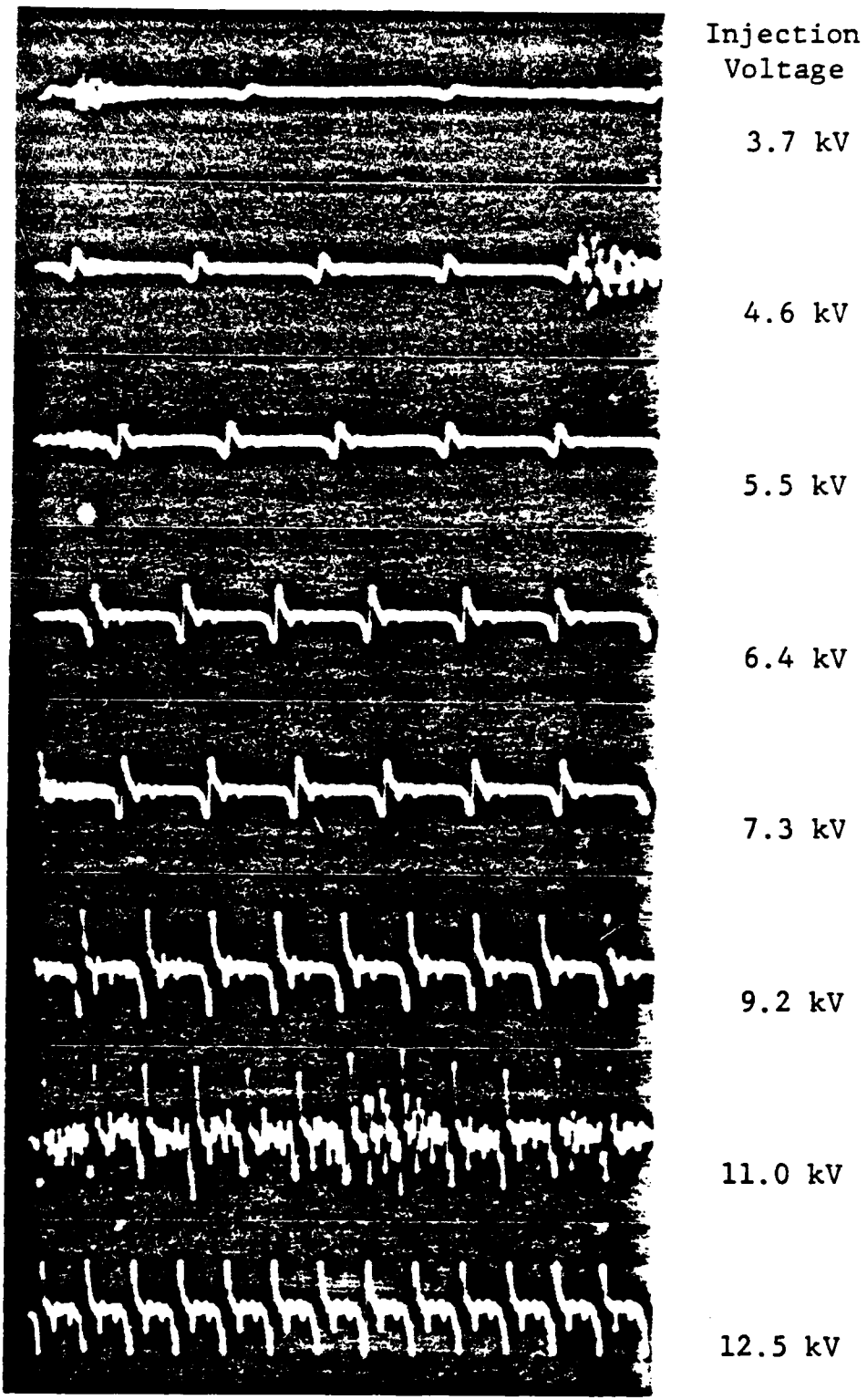
The mirror ratio changes with time. Figure 9a shows the current which flows through one section of the toroidal coils. Figure 9b is the current in one of the closed loops. These waveforms indicate, roughly speaking, that the mirror ratio decreases rapidly after the time when the toroidal field reached its peak. An X-ray burst appears soon after this time as shown in Figure 9c. Electrostatic oscillations were not observed afterwards.

#### 1-7 FOUR MIRROR EXPERIMENT

The injectors used in the four mirror experiment were not all of the same design. Two of the injectors ( $\theta = 0^\circ$ ,  $135^\circ$ ) gave electron trapping in wide ranges of the experimental parameters, but the other two ( $\theta = 180^\circ$ ,  $315^\circ$ ) worked in very limited ranges. This made the simultaneous trapping in four mirrors difficult and unrepeatable. Insufficient time and resources were available to fabricate new injectors of a common design.

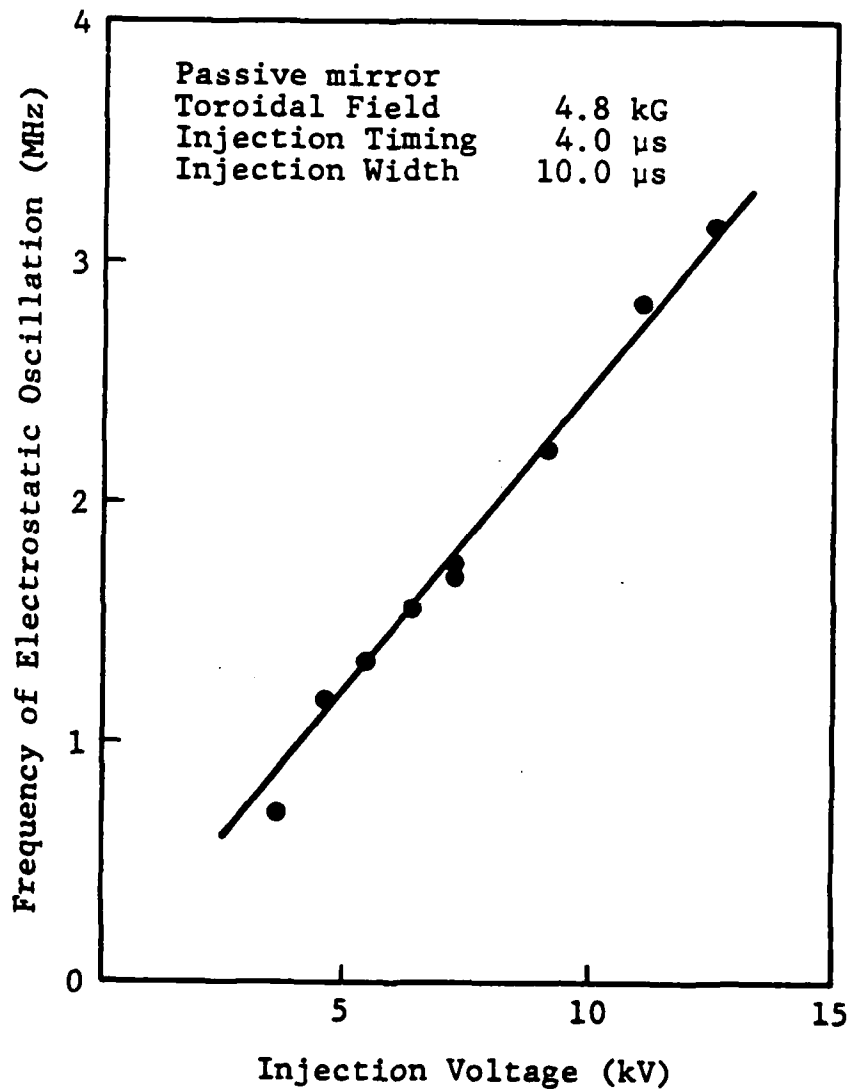
In addition to electrostatic probe measurements in the mirror cells, the electrostatic oscillations were detected by an electrostatic probe located halfway between  $\theta = 135^\circ$  and  $180^\circ$ . The frequency measured between the cells was the same as





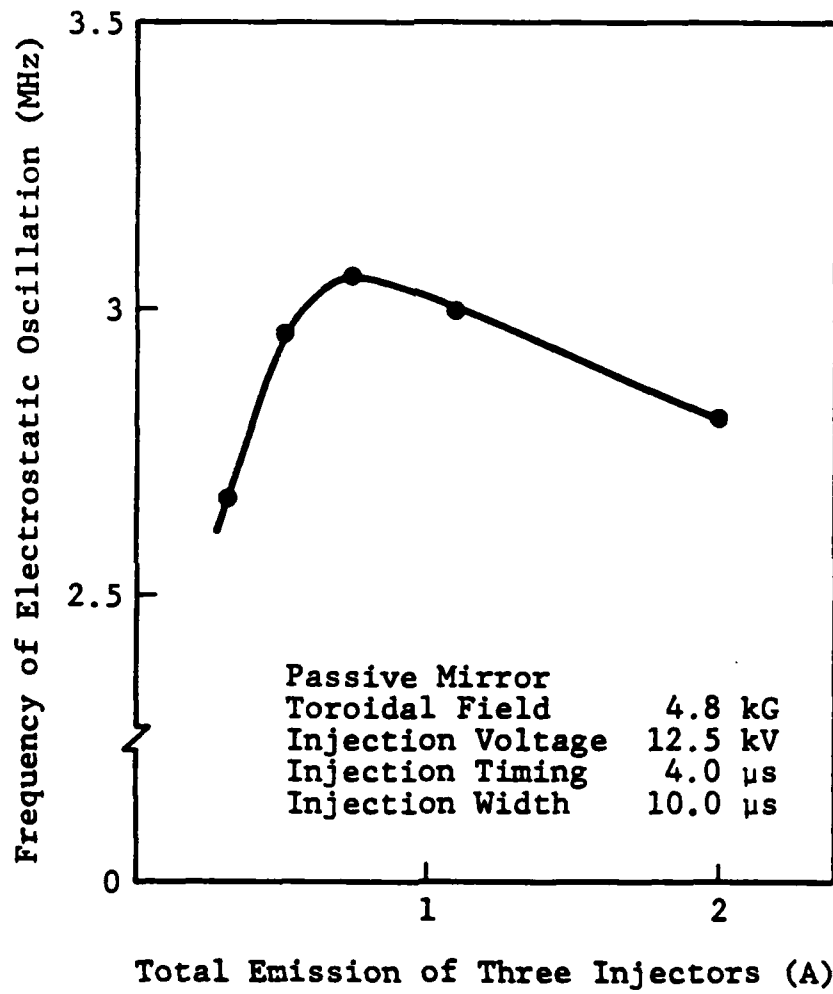
MLI82-411

Figure 6. Oscilloscope traces of electrostatic oscillations for different injection voltages.



MLI82-412

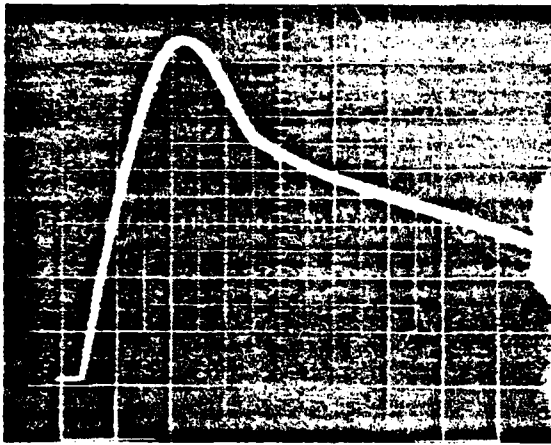
Figure 7. Injection voltage dependence of the electrostatic oscillation.



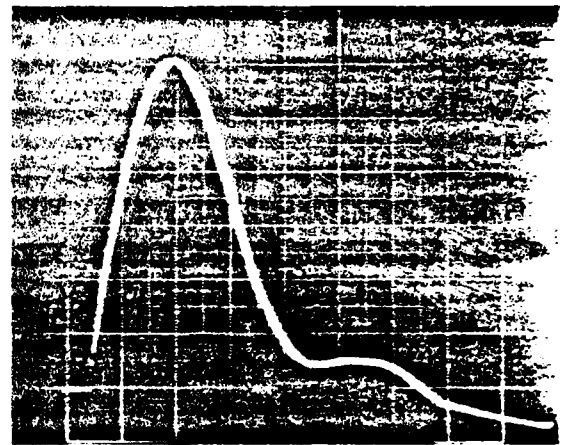
Total Emission of Three Injectors (A)

MLI82-413

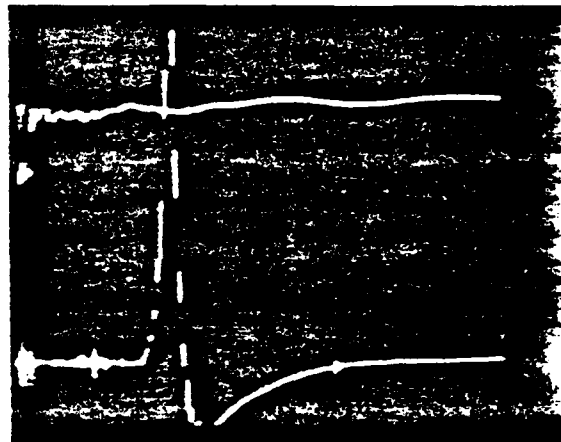
Figure 8. Frequency of electrostatic oscillation as a function of injected current.



(a) Current in the toroidal coil.



(b) Current in a closed loop.



(c) Upper trace: injected current (first 10  $\mu$ s).  
Lower trace: X-rays.  
50  $\mu$ s/div.

MLI82-414

Figure 9. Waveforms from toroidal experiment.

that measured at  $\theta = 180^\circ$  within the limits of experimental error and repeatability.

#### 1-8 DISCUSSION

The process of injection has been verified for a small number of mirrors. The present experiment is limited to magnetic fields between 3.5-7.0 kG and a small number of injector/mirrors. Electrons are trapped and contained as expected in the mirror fields. However, when the mirror fields are relaxed there is insufficient charge to avoid the toroidal drift. (This is consistent with estimates of the line density of the injected charge as determined from the diocotron oscillations.) As a result, the electrons drifted to the walls when the mirror fields were relaxed instead of being contained in the torus.

This research will continue under ONR sponsorship. Some of the limitations of the experimental apparatus relating to power conditioning, coil design, etc., will be improved. Thus far, no new physics problems have arisen and the principles of the injection/trapping scheme have been documented.

A continuous theoretical effort has been carried out. The main results to date are a comprehensive analysis of the problems of orbital stability that are presented in Appendix B.

## LIST OF APPENDICES

- A. High Current Betatron, G. Barak, D. Chernin, A. Fisher, H. Ishizuka, and N. Rostoker, Proceedings of the IV Conference on High Power Electron and Ion Beams, Palaiseau, France, June 1981.
- B. Orbital Stability of the High Current Betatron, G. Barak and N. Rostoker, submitted to Physics of Fluids.

APPENDIX A  
HIGH CURRENT BETATRON

## HIGH CURRENT BETATRON\*

G. Barak, D. Chernon, A. Fisher, H. Ishizuka, and N. Rostoker  
University of California, Irvine, California, and  
Maxwell Laboratories, Inc., San Diego, California

### ABSTRACT

In a conventional Betatron, space charge limits the electron current during injection. By adding a toroidal magnetic field and injecting electrons with the inductive charging method we expect to increase the current limit by a factor of  $10^4 - 10^6$ . After the beam has been accelerated to high energy the toroidal field is no longer necessary and can be reduced to facilitate extraction of the beam. The effect of the toroidal magnetic field on space charge instabilities is investigated. An experimental Betatron has been constructed with a major radius of 40 cm and a minor radius of 5 cm. On the basis of previous experimental results with inductive charging the current limit should be a few kilo-amperes.

### I. INTRODUCTION

In a conventional Betatron the orbit radius is  $R = \gamma mc^2 \beta / eB_y$  where  $B_y$  is the Betatron field,  $\beta = v/c$  and  $\gamma = (1 - \beta^2)^{-1/2}$ . For the usual injector<sup>1</sup>  $\gamma = 1$ ,  $\beta < 1$ ; for example, with a 100 keV injector and  $R = 1$  meter,  $B_y = 10.6$  gauss. The space charge current limit is proportional to  $B_y^2$ , and is therefore very small.

The current limit has been increased by reducing the orbit radius and increasing the injection energy.<sup>2</sup> Another proposal to eliminate the space charge problem by introducing a plasma was not successful.<sup>3</sup> Controlling space charge of electrons by adding a toroidal magnetic field to the usual Betatron fields was first investigated theoretically<sup>4</sup> in 1973, and the first experiments were reported<sup>5</sup> in 1976. A similar proposal for ions was made in 1978.<sup>6</sup>

During the past five years the technology of inductive charging has been developed at U.C.I. in experiments with magnetic mirrors<sup>7</sup> and a bumpy torus.<sup>8</sup> A line density of  $4 \times 10^{11}$  electrons/cm has been injected and confined for several milliseconds.<sup>8</sup> A new Betatron experiment has been constructed during the past year. It is illustrated schematically in Fig. 1. A local mirror is created into which injection and trapping take place, exactly as in the previously studied bumpy torus. However, the diamagnetic current in the copper ring (washer) decays on a short time scale compared to the toroidal magnetic field. The electrons trapped in the mirror are then ejected along the field lines as the mirror collapses. Based on the results with the bumpy torus we expect to trap enough electrons to produce a current of



a few kilo-amperes when the electrons are accelerated to  $\beta = 1$ . Various instabilities may arise in the modified Betatron including space charge, negative mass, resistive wall and orbital resonance instabilities. In general the toroidal magnetic field is stabilizing. In this paper we shall consider only space charge instabilities; the other instabilities have been considered in previous publications.<sup>9,10</sup> Space charge instabilities have previously been discussed for the field index  $s = \frac{1}{2}$  which is a special case in which the analysis is simple. The present analysis includes  $s \neq \frac{1}{2}$  and a consideration of electric and magnetic images.

## II. SPACE CHARGE INSTABILITIES

To describe the orbits in a toroidal electron beam consider the local coordinates  $(x, y)$  or  $(r, \theta)$  illustrated in Fig. 2. The equations of motion for standard Betatron fields  $B_y = B_0 (1 + \frac{sx}{R})$ ,  $B_x = \frac{sB_0}{R} y$  and a toroidal field  $B_z$ , are as follows<sup>9</sup>

$$\ddot{x} + \frac{\dot{\gamma}}{\gamma} \dot{x} + \Omega_z \dot{y} + [(1-s)\Omega_y^2 - \Omega^2] x = -\frac{\Omega_z}{2} \frac{\dot{B}_z}{B_z} y \quad (1)$$

$$\ddot{y} + \frac{\dot{\gamma}}{\gamma} \dot{y} - \Omega_z \dot{x} - [s\Omega_y^2 - \Omega^2] y = \frac{\Omega_z}{2} \frac{\dot{B}_z}{B_z} x \quad (2)$$

$\Omega_z = eB_z/\gamma mc$ ,  $\Omega_y = eB_0/\gamma mc$ ,  $\Omega^2 = \omega_p^2/2\gamma^2$  where  $\omega_p^2 = 4\pi ne^2/\gamma m$  and  $s$  is the field index.  $(x, y)$  describe oscillations about the equilibrium orbit given by the Betatron condition  $R = v_z/\Omega_y$  where  $v_z \approx c$  is the velocity of the electron in the toroidal direction.

For the special case  $s = .5$  these equations may be combined via the transformation

$$\xi = (x + iy) \gamma^{\frac{1}{2}} \exp\left[-\frac{1}{2} \int_0^t dt' \Omega_z(t')\right] \quad (3)$$

to give  $\ddot{\xi} + \omega^2 \xi = 0$  where

$$\omega^2 = \frac{1}{2} \Omega_y^2 - \Omega^2 + \frac{\Omega_z^2}{4} - \frac{1}{4} \left(\frac{\dot{\gamma}}{\gamma}\right)^2 - \frac{1}{2} \frac{d}{dt} \left(\frac{\dot{\gamma}}{\gamma}\right) \quad (4)$$

Transverse beam stability requires  $\omega^2 > 0$ . For a coasting beam ( $\dot{\gamma} = 0$ ) this corresponds to

$$n < \frac{\gamma}{4\pi mc^2} (B_y^2 + \frac{1}{2} B_z^2) \quad (5)$$

The advantage of using a strong toroidal field is apparent when  $\gamma \approx 1$  and  $B_y$  is small. After acceleration when  $\gamma$  and  $B_y$  are large the toroidal field can be permitted to decay to facilitate beam extraction.

The limiting current is determined by the injection conditions. For a con-

ventional Betatron  $n < \gamma B_y^2 / 4\pi mc^2$  implies a maximum current

$$I_m = (17/4) \gamma^3 \beta^3 (r_b/R)^2 \text{ k-amps} \quad (6)$$

For the modified Betatron with a toroidal field

$$I_m = (17/8) \gamma^3 \beta^3 (r_b/R)^2 (B_z/B_0)^2 \text{ k-amps} \quad (7)$$

where we have used the Betatron condition  $R = \beta c / \Omega_y$ .

If  $s$  is not exactly .5 the general solution of Eqs. (1) and (2) gives three independent conditions that must be satisfied.

$$(\omega_x^2 + \omega_y^2 + \Omega_z^2)^2 > 4\omega_x^2 \omega_y^2 \quad (8)$$

$$\omega_x^2 \omega_y^2 > 0 \quad (9)$$

$$\omega_x^2 + \omega_y^2 + \Omega_z^2 > 0 \quad (10)$$

where  $\omega_x^2 = (1-s)\Omega_y^2 - \Omega^2$ ,  $\omega_y^2 = s\Omega_y^2 - \Omega^2$  and  $\omega^2 = \frac{\omega_x^2 + \omega_y^2}{2} + \frac{\Omega_z^2}{4}$ . We have assumed  $s$ ,  $\gamma$ ,  $\Omega_z$ ,  $\Omega_y$  and  $\Omega$  are time independent. Equations (8) and (10) are satisfied if  $\omega^2 > 0$ . However Eq. (9) is independent of  $\Omega_z$ . This condition is illustrated in Fig. 3 where  $(\Omega_z/\Omega_y)^2$  is plotted against  $s$  and the stable region is indicated. In the lower region conventional Betatrons operate and  $\omega_x^2, \omega_y^2 > 0$ . In the high current Betatron, the initial operating point is in the upper region, but as  $\gamma$  rises we eventually must cross the unstable region except for  $s = 1/2$ . In the unstable region the beam will expand,  $\Omega^2$  will drop and a transition to the lower stable region will occur. For example, if  $s = \frac{1}{2}(1+\delta)$  the density drop will be  $\Delta n/n \approx 2|\delta|$ . If  $N$  is the line density and  $r_b$  is the beam radius the transition occurs for  $\gamma$  such that  $\gamma^3 \beta^2 > 4Nr_e (R/r_b)^2$  where  $r_e$  is the classical electron radius. Assuming  $N = 10^{11} \text{ cm}^{-1}$ ,  $R = 40 \text{ cm}$ ,  $r_b = 1 \text{ cm}$  the transition takes place at  $\gamma \approx 6$ .

The Fermi drift has not been included in Eqs. (1) and (2). The Fermi drift is due to the fact that the toroidal field is not constant; i.e.,  $B_z = B_{z0} [1 + \frac{x}{R}]$  so that the drift velocity is  $\dot{y} \approx v_{\perp}^2 / 2 \cdot \Omega_z R$ . In Eq. (1)  $\Omega_z \dot{y}$  must be replaced by  $\Omega_{z0} [1 + \frac{x}{R}] \dot{y}$ . The Fermi-drift term  $\Omega_{z0} x \dot{y} / R$  is non-linear. It may be compared to the term  $\Omega^2 x$  or  $(1-s)\Omega_y^2 x$ . In the first case if

$$\frac{\Omega_{z0} \dot{y} / R}{\Omega^2} = \frac{\dot{y}}{\omega_0 R} = \frac{\gamma^2}{R^2} \left( \frac{v_{\perp}}{\omega_p} \right)^2 \ll 1$$

the Fermi drift term can be neglected. Physically the drift is corrected by the self-field drift which causes angular rotation at the frequency

$\omega_0 = \Omega^2 / \Omega_{z0}$ . The displacement due to Fermi drift  $\dot{y}/\omega_0$  is negligible for a dense beam and small  $\gamma$ . If  $\gamma$  is large the self electric and magnetic fields almost cancel. However, in that case the Fermi drift may still be neglected if

$$\frac{2\Omega_{z0} \dot{y}/R}{\Omega^2} = (p_{\perp}/\gamma mc)^2 \ll 1$$

In this case the Fermi drift is compensated by the focusing effect of the Betatron field. The Fermi drift may be neglected except when  $(1-s)\Omega_y^2 - \Omega_x^2 = \omega_x^2 \approx 0$ . This is an unstable region in any case and should be passed quickly as discussed above.

If the electron ring is in a conducting torus, but displaced from the axis, electric and magnetic images at the wall will create forces on the beam that cause it to drift. Equations of motion for the center of mass of the beam moving in external fields including image fields are similar to Eqs. (1) and (2). The results are formally the same with the revised definitions

$$\begin{aligned} \omega_x^2 &= (1-s)\Omega_y^2 - (r_b/a)^2 \Omega^2 \\ \omega_y^2 &= s\Omega_y^2 - (r_b/a)^2 \Omega^2 \\ \Omega^2 &= \omega_p^2/2 \end{aligned}$$

We have assumed that image currents in the wall decay immediately and image charges survive.  $r_b$  is the beam radius and  $a$  is the minor radius of the torus.

The beam will drift around the toroidal axis. As  $\gamma$  increases it must pass through an unstable region when  $\gamma\beta^2 = 4Nr_e(R/a)^2$ . For  $N = 10^{11} \text{ cm}^{-1}$ ,  $R = 40 \text{ cm}$  and  $a = 5 \text{ cm}$ ,  $\gamma \approx 8$ . In this case the self field term  $r_b^2 \Omega^2/a^2$  depends only on line density which is not altered by the instability. It is necessary to have  $s \approx 1/2$  and to change  $\gamma$  rapidly enough that the beam does not displace to the wall.

The unstable region for beam motion is not the same as the unstable region for single particle orbits. In the neighborhood of the latter unstable region the Fermi drift is significant. The beam drift due to electrostatic image forces should then be considered. The drift frequency is  $\omega_0 = (r_b^2 \gamma^2/a^2) \Omega^2 / \Omega_{z0}$  where  $\Omega^2 = \omega_p^2/2\gamma^2$ . The Fermi drift may be neglected if

$$\frac{\dot{y}}{\omega_0 R} = \frac{a^2}{r_b^2} \frac{(v_{\perp}/\omega_p)^2}{R^2} \ll 1$$

### III. EXPERIMENTAL PARAMETERS

An experiment has been constructed with the objective of producing a 1 k-ampere beam of electrons at 10 MeV. The torus is a glass chamber with a metal screen liner of major radius 40 cm and minor radius 5 cm. A vacuum of  $5 \times 10^{-8}$  torr has been achieved with a cryo-pump. The toroidal magnetic field has a peak value of 12 k-Gauss with a rise time of 100  $\mu$ sec. After crow-barring the decay time is about 300  $\mu$ sec. The Betatron field has a peak value of 1 k-Gauss at the major radius with a rise time of 350  $\mu$ sec. The field index varies from .2 to .8 in the chamber. Magnetic field errors have been determined to be less than 1%. Injectors are similar to those previously employed in the bumpy torus.<sup>8</sup> They operate at 15 k-volts with a current at 5 amps. for 5  $\mu$ sec. They have been operated at voltages as high as 30 k-volts. Construction and field measurements were completed in May 1981 and injection experiments are now in progress. Figure 4 is a photograph of the U.C.I. Betatron experiment.

\*Work supported by the Defense Advance Research Project Agency and the Office of Naval Research.

We are indebted to Donald W. Kerst for many illuminating discussions.

### REFERENCES

1. D. W. Kerst, G. D. Adams, H. W. Koch, and C. S. Robinson, Phys. Rev. 78, 297 (1950).
2. A. I. Pavlovski, G. D. Kuleshov, G. V. Sklizkov, Y. A. Zysin, and A. I. Gerasimov, Sov. Phys. Tech. Phys. 22, 210 (1977).
3. G. I. Budker, CERN Symposium 1, 68 (1956); 1, 76 (1956); P. Reynolds and H. M. Skarsgard, J. Nucl. Energy C1, 36 (1960).
4. N. Rostoker, Particle Accelerators 5, 93 (1973).
5. W. Clark, P. Korn, A. Mondelli, and N. Rostoker, Phys. Rev. Lett. 37, 592 (1976).
6. P. Sprangle and C. A. Kapetanacos, J. Appl. Phys. 49, 1 (1978).
7. S. Eckhouse, A. Fisher, and N. Rostoker, Phys. Fluids 21, 1840 (1978).
8. A. Fisher, P. Gillad, F. Goldin, and N. Rostoker, Appl. Phys. Lett. 36, 264 (1980); 37, 531 (1980).
9. N. Rostoker, Comments on Plasma Physics 6, 91 (1980).
10. G. Barak, A. Fisher, H. Ishizuka, and N. Rostoker, I.E.E.E. Trans. Nuc. Sc. NS-28, 3340, 1981.

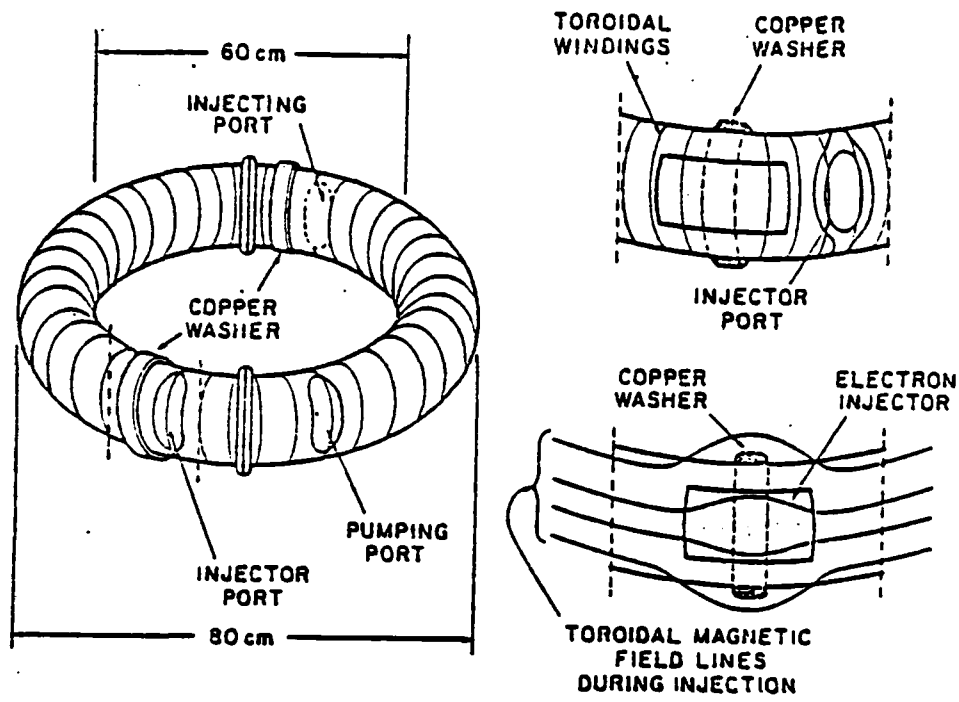


Figure 1. Betatron Experiment

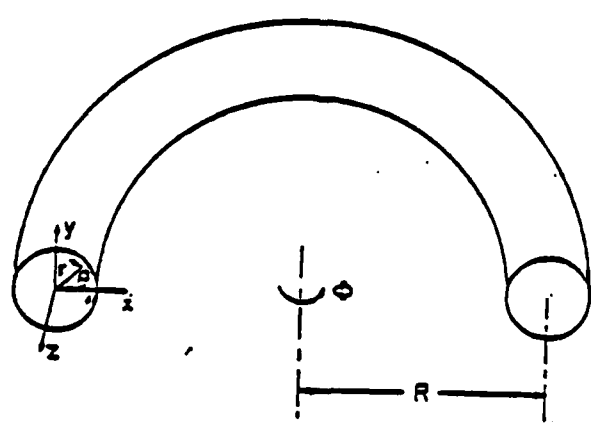


Figure 2. Coordinates for a Toroidal Electron Beam

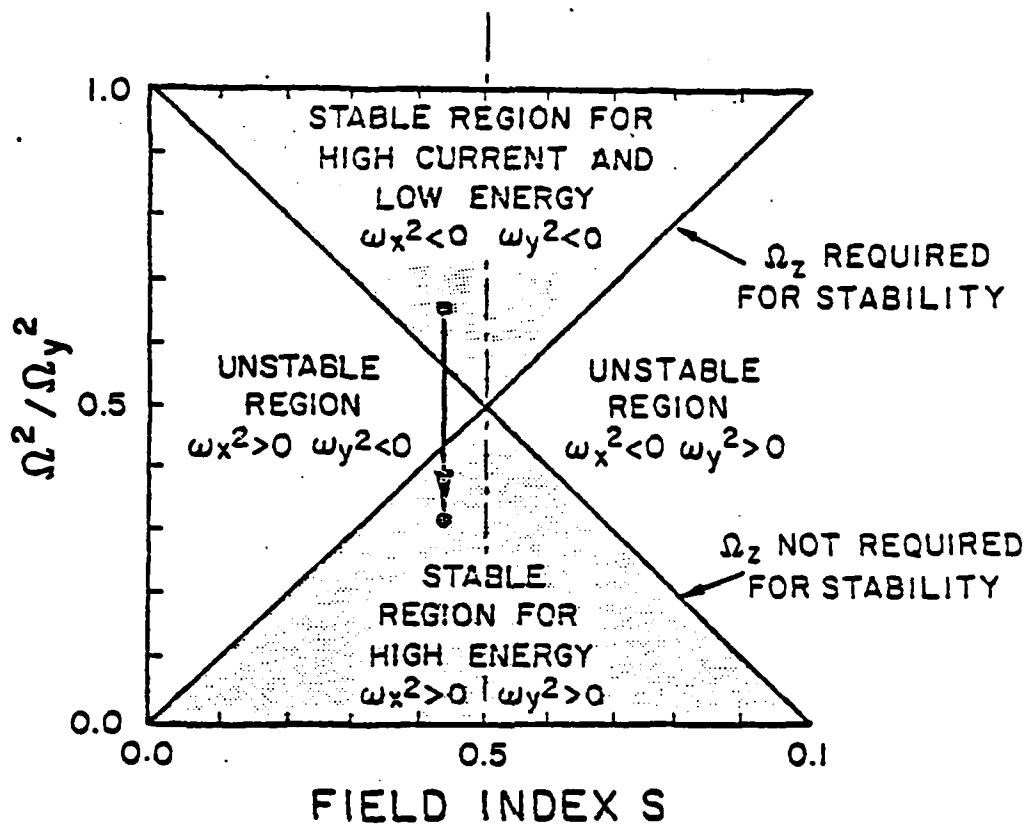


Figure 3. Stability condition for the modified Betatron. Initial and final operating points are indicated. The transition takes place when  $\gamma$  is increased or  $n$  decreases.

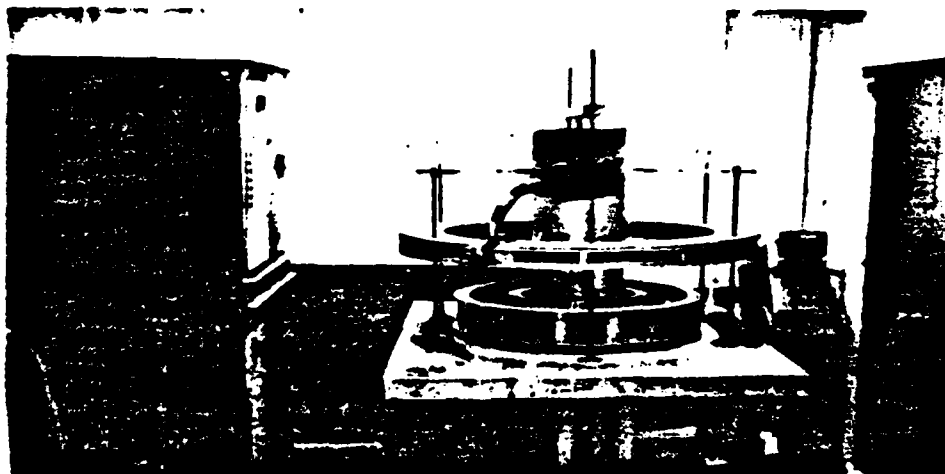


Figure 4. U. C. I. Betatron Experiment

APPENDIX B

ORBITAL STABILITY OF THE HIGH CURRENT BETATRON

# ORBITAL STABILITY OF THE HIGH CURRENT BETATRON

by

G. Barak and N. Rostoker

Department of Physics  
University of California  
Irvine, California 92717

UCI Technical Report #81-91

December 1981

## Abstract

We analyze orbital stability of the High Current Betatron. In this modified Betatron a toroidal magnetic field is added to the conventional Betatron magnetic field. This increases substantially the space charge limit during injection. It gives rise, however, to new problems during acceleration, such as ring stability, Fermi drift and orbital resonances. A detailed analysis is presented showing that two serious problems may arise; (i) The beam becomes highly unstable when the net focusing force on it becomes zero. The dominant instability in this region is the Fermi drift. This may, however, be utilized in extracting the beam. (ii) Errors in the vertical (Betatron) magnetic field result in driven resonances that must be crossed during acceleration. The amplitude growth of the transverse Betatron oscillations due to these resonances is negligible up to very high  $\gamma$  (low  $n$  resonances). It may become practically very difficult to cross the  $n=1$  resonance. Thus again extracting the beam by making use of the Fermi drift while  $n > 1$  is preferable.



## I. INTRODUCTION

The largest conventional Betatron was completed about 1950.<sup>1</sup> The energy was about 300 MeV and the beam current about 100 milliamperes. The maximum beam current was limited by space charge during injection. Electrons from a 100 KeV electron gun were injected into an orbit of radius  $R \approx 1$  meter and a Betatron magnetic field of  $B_y \approx 10$  Gauss. The space charge limit is proportional to  $B_y^2$  and for the Kerst Betatron<sup>1</sup>  $n \leq 10^7 \text{ cm}^{-3}$ . The space charge limit is also proportional to  $\gamma$ , thus it is greatly increased after acceleration. In a conventional Betatron it is the space charge limit at injection which determines the maximum current.

To eliminate the space charge problem the plasma Betatron was proposed by Budker.<sup>2</sup> After many studies<sup>3</sup> were carried out, the maximum current reached about 10 amperes, much less than expected. The current is probably instability limited. The precise instability has not been identified, although the negative mass instability is mentioned frequently.<sup>4</sup>

By increasing the injection energy and decreasing the orbit radius in a conventional Betatron, the space charge limit can be increased ( $n \approx \beta^2 \gamma^3 / R^2$ ). Small "ironless" Betatrons have been developed with an electron energy of 100 MeV and electron currents of about 90 amperes.<sup>5</sup> Electrons were injected into a 3.9 cm orbit radius with energy of 500 KeV. The space charge limit was increased by a factor of  $\sim 10^4$  compared to the Kerst Betatron. The total number of electrons was increased however, only by a factor of  $\sim 40$ .

Controlling space charge of electrons by adding a toroidal magnetic field to the usual Betatron field was first investigated theoretically<sup>11</sup> in 1973 and the first experiments were reported<sup>10</sup> in 1976. A similar proposal for ions was made in 1978.<sup>12</sup>

The combined toroidal and vertical (Betatron) fields increase substantially the space charge limit and the number of electrons that can be trapped and accelerated. Injecting and trapping into such combined fields require new techniques. Several methods were proposed lately.<sup>6,7</sup> The first method<sup>6</sup> has already been demonstrated in the studies of the Collective Focusing Ion Accelerator.<sup>8</sup> The method is called inductive charging and was first used in HIPAC.<sup>9</sup> Electrons are injected from thermionic injectors and trapped by means of a rising toroidal magnetic field. A Betatron with this type of injection is illustrated in Figure 1. Electrons move in an orbit around the torus. They are not drifted in the toroidal field due to the self field forces and the interaction with the surrounding metallic boundaries. There are no restrictions on  $B_z$  as there are on  $B_y$  in a conventional Betatron. As the space charge limit depends on  $B_z^2$  during injection, a substantial increase in the density can be achieved. With the existing injectors, the current after acceleration will be  $\sim 1$  KAmper.<sup>8</sup> Better injectors may increase this current further by 1-2 orders of magnitude.

The toroidal magnetic field solves the problem of increasing the space charge limit during injection. It creates, however, new problems during acceleration. It is the purpose of this paper to investigate the regions of instability of this high current

Betatron and to suggest an optimum mode of operation. We shall assume throughout this paper that inductive charging is used. The parameter set we shall use as a standard reference is given in Table 1. We shall discuss only orbital instabilities. Collective instabilities, such as negative mass, or resistive wall instabilities have not been treated in this paper, but it is known<sup>13</sup> that toroidal field decreases their importance.

## II. SINGLE PARTICLE ORBITS

### 2.1 Equations of Motion

In order to describe the particle orbit in a toroidal electron beam, consider the local coordinates  $(x,y)$  or  $(r,\theta)$  as illustrated in Fig. 2. The toroidal direction is indicated by  $z$ . If  $\Omega_y = \frac{eB_y}{\gamma mc}$  electrons will move on a radius  $R = \frac{v_z}{\Omega_y}$ . Furthermore, if  $B_y$  is changed in time so that

$$B_y(R) = \frac{1}{2R^2} \int_0^R B_y(r) r dr$$

the electrons will move on a constant radius. Due to the beam self fields and the distribution of the initial conditions electrons will also move in the transverse directions. This motion determines the maximum current that can be obtained and the quality of the beam. The equations of motion, up to first order in  $(x/R)$ , where  $x$  is the deviation from the Betatron equilibrium orbit, are:

$$m\gamma \left[ \ddot{x} + \dot{y} \dot{x} + \frac{v_z^2}{R-x} \right] = -e \left[ (E_r - \beta B_\theta) \frac{x}{R} + \frac{1}{c} (v_y B_z - v_z B_y) \right] \quad (2.1)$$

$$m\gamma \left[ \dot{y} + \dot{y} y \right] = -e \left[ (E_r - \beta B_\theta) \frac{y}{R} + \frac{1}{c} (v_z B_x - v_x B_z) \right]$$

$B_z$  and  $B_y$  are the applied toroidal and vertical fields,  $E_r$  and  $B_\theta$  are the self fields. Interaction with the surrounding wall was neglected here and will be considered separately later. The equilibrium orbit is determined by the relation  $B_y(R) = \frac{1}{2} \bar{B}_y(R)$ .  $\bar{B}_y(R)$  is influenced by the beam current. For a high current Betatron this is not negligible, especially for the early stage of acceleration.

External currents should be added to eliminate this effect. We shall assume that this is done so that  $v_z = R\Omega_y$ , where  $R$  is constant and  $v_z \approx c$  (the case of  $\gamma \approx 1$  will be investigated separately).

For a cylindrical symmetric beam the self-fields are easily calculated,

$$-e(E_r - \beta B_\theta)/m\gamma r = \frac{\omega_p^2}{2\gamma^2} \cdot \frac{n(r)}{n}$$

where  $\frac{\omega_p^2}{\gamma^2} = \frac{4\pi n e^2}{\gamma m}$ ,  $n$  is the average density of the beam and  $n(r)$  is the average density up to radius  $r$ . If the beam is uniform,  $n(r)/n = 1$ , and the self force is harmonic.

The Betatron field is

$$B_y = B_0 \left(\frac{R}{R-x}\right)^s \approx B_0 \left(1 + \frac{sx}{R}\right) \quad (2.2)$$

$$B_x \approx \frac{s B_0 y}{R}$$

Thus we get the following equations of motion:

$$\ddot{x} + \dot{x} \frac{\dot{y}}{y} + \Omega_z \dot{y} + [(1-s)\Omega_y^2 - \Omega^2] x = 0 \quad (2.3)$$

$$\ddot{y} + \dot{y} \frac{\dot{y}}{y} - \Omega_z \dot{x} + [s\Omega_y^2 - \Omega^2] y = 0$$

where  $\Omega_z = \frac{eB_z}{\gamma mc}$ ,  $\Omega_y = \frac{eB_0}{\gamma mc}$ ,  $\Omega^2 = \frac{\omega_p^2}{2\gamma^2}$ .

The toroidal field was assumed constant. Higher order corrections will be discussed later.

## 2.2 Space Charge Limits

Define

$$\omega_x^2 = (1-s) \Omega_y^2 - \Omega^2 \quad (2.4)$$

$$\omega_y^2 = s \Omega_y^2 - \Omega^2$$

and assume that  $s$ ,  $\gamma$ ,  $\Omega_z$ ,  $\Omega_y$ ,  $\Omega$  are time independent. The general solution of Eqs. (2.3) and (2.4) can be expressed as a sum of two oscillations having frequencies

$$\omega_{1,2}^2 = \frac{\Omega_z^2 + \omega_x^2 + \omega_y^2 \pm (\Omega_z^2 + \omega_x^2 + \omega_y^2)^2 - 4\omega_x^2 \omega_y^2}{2}^{1/2} \quad (2.5)$$

Orbits are stable if and only if:

$$(a) \quad (\omega_x^2 + \omega_y^2 + \Omega_z^2)^2 > 4\omega_x^2 \omega_y^2$$

$$(b) \quad \omega_x^2 \omega_y^2 > 0 \quad (2.6)$$

$$(c) \quad \omega_x^2 + \omega_y^2 + \Omega_z^2 > 0$$

Denoting  $s = 1/2(1+\delta)$  these conditions can be written as:

$$(a) \quad (\Omega_z^2 + 2\Omega_y^2 - 4\Omega^2) \Omega_z^2 + \delta^2 \Omega_y^4 > 0.$$

$$(b) \quad [(\Omega/\Omega_y)^2 - 1/2]^2 > \frac{1}{4} \delta^2 \quad (2.7)$$

$$(c) \quad \Omega_z^2 + \Omega_y^2 - 2\Omega^2 > 0$$

Condition (b) involves only  $\Omega$  and  $\Omega_y$ . For  $\delta = 0$  it is always satisfied. When  $\delta \neq 0$  it is satisfied in two disconnected regions:

$$\left(\frac{\Omega}{\Omega_y}\right)^2 < \frac{1 - |\delta|}{2} \quad \text{or} \quad \left(\frac{\Omega}{\Omega_y}\right)^2 > \frac{1 + |\delta|}{2} \quad (2.8)$$

The first is the "low density" region in which conventional Betatrons are operated ( $\omega_x^2, \omega_y^2 > 0$ ). The second is the "high density" region ( $\omega_x^2, \omega_y^2 < 0$ ). In the high current Betatron we intend to start in the high density region, but as  $\gamma$  rises we eventually have to cross the unstable region (see Fig. 3). Here, the beam will start to expand, but as it expands  $\Omega^2$  will drop and a transition to the lower stable region will occur. An upper limit estimate of the density drop is  $|\frac{\Delta n}{n}| < 2|\delta|$ , thus for  $|\delta| \approx 0.25$  the beam will expand by less than 25% in radius.

This effect can be decreased by crossing the unstable region quick enough; e.g., by a rapid change of  $\gamma$ .

Conditions (a) and (c) are satisfied for every  $\delta$  if they are satisfied for  $\delta = 0$  ( $s = 1/2$ ). Condition (a) is then stronger than (c). Thus we get:

$$\Omega^2 < \frac{\Omega_z^2}{4} + \frac{\Omega_y^2}{2} \quad \text{or}$$

$$n < \gamma \left[ \frac{B_y^2}{4\pi mc^2} + \frac{B_z^2}{8\pi mc^2} \right] \quad (2.9)$$

For the inductive charging  $B_y \ll B_z$  at injection, thus  $n_{\max} \propto \gamma B_z^2$ . In experiments at the University of California, Irvine, electron ring of line density  $\sim 2 \cdot 10^{11} \text{ cm}^{-1}$  was injected and trapped. This corresponds to a current after acceleration of about 1 Kamp, and is larger by a factor of  $10^4$

compared to the Kerst Betatron. This is still two orders of magnitude less than the current that can be contained by a 10 kG toroidal field. We expect to increase the density of the trapped electron ring by using higher injection voltage which is presently 10 K-volts. In experiments at Maxwell Laboratories a line density of  $2.10^{12}$  was observed with an injector voltage of 30 K-volts.<sup>10</sup>

During acceleration  $\gamma B_y^2$  rises, thus if Eq. (2.9) is satisfied during injection it will be also satisfied during acceleration.

The transition from the high  $\Omega/\Omega_y$  region to the low  $\Omega/\Omega_y$  region occurs at

$$\gamma^3 \beta^2 = \frac{4NR^2 r_c}{r_b^2} \quad (2.10)$$

where  $r_c$  is the electron classical radius and  $r_b$  is the beam radius. For our standard example (Table 1) this means  $\gamma \approx 13$  and  $B_y \approx 210$  Gauss.



### III. RING ORBITS

Assume that the electron ring is shifted away from the axis of the torus. Electric and magnetic images at the wall will push the beam further onto the wall. Together with the toroidal magnetic field a slow rotation ( $\bar{\mathbf{F}} \times \bar{\mathbf{B}}$  drift) around the toroidal axis will start. We shall investigate here this transverse motion and find its stability regions. We shall consider only the z-independent mode, and expand the image forces to the lowest order in  $a/R_0$  (where  $a$  and  $R_0$  are the minor and major radii respectively).

To the lowest order in  $a/R_0$ , the image forces may be considered as created by an infinite cylinder of radius  $a$ . If the beam is off center by  $\delta x$  along the  $x$  axis, the image will be a line with the same line density  $N$  located at  $x = a^2/\delta x$ . The electric field at  $\delta x$  resulted by the image charge is

$$E_x = - \frac{2Ne}{|a^2/\delta x - \delta x|} = \frac{-2Ne\delta x}{a^2} \quad (3.1)$$

and the force exerted on an electron at  $\delta x$  will be:

$$F = \gamma m \Omega^2 (r_b/a)^2 \delta x \quad (3.2)$$

where

$$\Omega^2 = \frac{\omega_p^2}{2} = \frac{2\pi n e^2}{\gamma m}$$

The magnetic field depends on the image currents. If the wall is an ideal conductor the magnetic force is opposite to the electric force and reduces it by a factor of  $\gamma^2$ . We shall assume the

other extreme case; i.e., immediate decay. The equations of motion for the beam center are:

$$\ddot{x} + \frac{\dot{y}}{\gamma} \dot{x} + \frac{v_z^2}{R_0 - x} = \Omega^2 \left( \frac{r_b}{a} \right)^2 x - \Omega_z \dot{y} + \frac{eB_y}{\gamma mc} v_z \quad (3.3)$$

$$\ddot{y} + \frac{\dot{y}}{\gamma} \dot{y} = \Omega^2 \left( \frac{r_b}{a} \right)^2 y + \Omega_z \dot{x} - \frac{eB_x}{\gamma mc} v_z$$

$x$  and  $y$  are measured relative to the toroidal axis. If the beam center is shifted relative to this axis, the equilibrium radius will be determined by a different condition than that of a single particle, namely  $R = v_z / \Omega_y(R)$ . This is due to the additional force in the  $x$  direction. Assume that the equilibrium orbit,  $R$ , is shifted in the  $x$  direction by  $\delta x$ ; i.e.,  $R = R_0 - \delta x$ . If the Betatron field is expanded around  $R$  we get:

$$B_y \approx B_0 \left[ 1 + s \frac{x - \delta x}{R} \right] \quad (3.4)$$

$$B_x \approx B_0 \frac{sy}{R}$$

Note that  $v_z = R \Omega_y(R)$  and  $s = s(R)$ ,  $B_0 = B_0(R)$ .

Substituting in Eq. (3.3) we get for the  $x$  component

$$\ddot{x} + \frac{\dot{y}}{\gamma} \dot{x} + \Omega_z \dot{y} + \left[ (1-s) \Omega_y^2 - \left( \frac{r_b}{a} \right)^2 \Omega^2 \right] x = - (s-1) \Omega_y^2 \delta x \quad (3.5)$$

If we make the transformation

$$x \rightarrow x - \frac{(s-1) \Omega_y^2 \delta x}{(1-s) \Omega_y^2 - (r_b/a)^2 \Omega^2} \quad (3.6)$$

which is permitted as long as the denominator is not zero, the equations of motion become:

$$\ddot{x} + \frac{\dot{y}}{y} \dot{x} + \Omega_z \dot{y} + \omega_x^2 x = 0 \quad (3.7)$$

$$\ddot{y} + \frac{\dot{y}}{y} \dot{y} - \Omega_z \dot{x} + \omega_y^2 y = 0$$

where

$$\omega_x^2 = (1-s)\Omega_y^2 - (r_b/a)^2 \Omega^2 \quad (3.8)$$

$$\omega_y^2 = s\Omega_y^2 - (r_b/a)^2 \Omega^2$$

The beam equilibrium radius is thus shifted by

$$\Delta x = \frac{(1-s)\Omega_y^2 \delta x}{(1-s)\Omega_y^2 - (r_b/a)^2 \Omega^2} \text{ relative to the toroidal axis. The}$$

physical reason for this is that the image force supplies part of the centripetal force.

Equations (3.7) are similar to Eq. (2.3). For  $s = 1/2$  the motion is stable if

$$\Omega^2 < \left(\frac{a}{r_b}\right)^2 \left[ \frac{\Omega_z^2}{4} + \frac{\Omega_y^2}{2} \right] \quad (3.9)$$

or

$$n < \frac{1}{\gamma} \left(\frac{a}{r_b}\right)^2 \left[ \frac{B_z^2}{8\pi mc^2} + \frac{B_y^2}{4\pi mc^2} \right]$$

This equation can be written approximately as:

$$N < \frac{4 \cdot 10^{14}}{\gamma} + 2 \cdot 10^9 \gamma$$

where  $N$  is the line density and the parameters of Table 1 were used. If  $N < 1.8 \cdot 10^{12}$ , the beam is stable for every  $\gamma$ . However, for  $N > 1.8 \cdot 10^{12}$  there is a region of instability. For  $N = 10^{13} \text{ cm}^{-1}$  this region starts already at  $\gamma = 40$ . To overcome it either  $B_z$  should be raised or the currents in the wall should persist longer.

Equations (3.7) have the same stability problem as we saw in Eq. (2.8). It will start at

$$\Omega^2 \approx \frac{1}{2} (a/r_b)^2 \Omega_y^2 \quad \text{or} \quad \gamma \beta^2 \approx 4N(R/a)^2 r_c \quad (3.10)$$

where  $r_c$  is the electron classical radius. For our standard parameters this will occur at  $\gamma \approx 90$ . In contrast to the single particle case, the self field depends here only on the line density, which does not change as the instability develops. It is thus necessary to cross this region fast enough. An estimate of the growth rate can be given at the maximum; i.e., at  $\Omega^2 = \frac{1}{2} (a/r_b)^2 \Omega_y^2$ . Here the e-folding time is

$$\frac{2\Omega_z}{|s - \frac{1}{2}| \Omega_y^2} \approx \frac{0.045}{|s - \frac{1}{2}|} \mu\text{sec}$$

which is much less than  $\mu\text{sec}$  unless  $|s - \frac{1}{2}| \ll 1$ .

Besides the exponential growing instability the beam will drift in the  $y$  direction. This is due to the r.h.s. term of Eq.

(3.5). The drift speed is  $\frac{1}{2} \frac{\Omega_y^2}{\Omega_z} \delta x \approx 20 \delta x \text{ cm}/\mu\text{sec}$ . Assuming  $\delta x = 0.5 \text{ cm}$  the beam will hit the wall in  $0.5 \mu\text{sec}$ . Increasing  $NR^2$  will increase the  $\gamma$  where the transition occurs. Thus the

instability may be avoided (if  $NR^2$  is large enough) or it may be used as a means to extract the beam.

In concluding this section a remark should be made concerning the single particle orbits. In Eqs. (2.1) we neglected the force created by the image charges. This force will add oscillating terms to Eqs. (2.3). A problem will arise only when the single electron and the beam motions are in resonance; i.e.,  $\omega^\pm(\text{single particle}) = \omega^\pm(\text{beam})$ . This is not likely to happen because the  $\omega_x^2$ ,  $\omega_y^2$  in Eqs. (2.4) and (3.8) are different (as long as  $\Omega$  is not very small compared to  $\Omega_z$ ).

## IV. BEAM EMITTANCE

The quality of a beam is sometimes described by its emittance, defined as:

$$\epsilon/\pi = \theta \rho = \bar{p}_\perp \epsilon/p_z \quad (4.1)$$

where  $\rho$  is the beam radius and  $\theta$  is the angular divergence. Emittance is determined mainly by the method of injection. For inductive charging  $\bar{p}_\perp \rho = m v_{10} a = \text{const}$ , where  $a \approx 5$  cm (the beam radius during injection), and  $v_{10}/c \approx 0.2$  corresponding to 10 keV injector. When the toroidal field reaches its maximum of  $\sim 10$  KGauss the beam radius is of the order of 1 cm and the transverse kinetic energy is  $\sim 500$  keV.<sup>8</sup> During acceleration  $\bar{p}_\perp = \text{const}$ , but  $\rho$  decreases due to the  $B_y$  increase and the self-pinching effect. For simplicity assume  $s = \frac{1}{2}$  and consider Eq. (2.3). If  $B_z$  is changing in time, the induced field  $E_\theta$  should be included. Transforming then to the rotating Larmor frame we get:

$$\ddot{u} + \dot{u} \frac{\dot{\gamma}}{\gamma} + \frac{1}{4} (\Omega_z^2 + 2\Omega_y^2 - 4\Omega^2) u = 0 \quad (4.2)$$

where

$$x + iy = \exp \left[ \frac{i}{2} \int_0^t \Omega_z(t') dt' \right] u(t)$$

This is correct for any change of  $\Omega_z$ ; either changing  $\gamma$  or  $B_z$ .

The mixed term  $\dot{u} \frac{\dot{\gamma}}{\gamma}$  can be eliminated by the transformation

$$u = \gamma^{-\frac{1}{2}} z \quad (4.3)$$

yielding

$$\ddot{z} + \omega^2 z = 0$$

where

$$\omega^2 = \frac{1}{4} \left[ \Omega_z^2 + 2\Omega_y^2 - 4\Omega^2 - \left( \frac{\dot{\gamma}}{\gamma} \right)^2 - 2 \frac{d}{dt} \left( \frac{\dot{\gamma}}{\gamma} \right) \right] \approx \frac{1}{4} \left[ \Omega_z^2 + 2\Omega_y^2 - 4\Omega^2 \right] \quad (4.4)$$

Eq. (4.3), for the real and imaginary parts of  $z$  can be solved using the WKB approximation. The general solution can be written as

$$z_i = \frac{c_i}{\sqrt{\omega}} \cos(\omega t + \varphi_i)$$

where  $c_i$  and  $\varphi_i$  are determined by the initial conditions, thus

$$r^2 = \gamma^{-1} |z|^2 = \frac{1}{\gamma \omega} [A^2 + B^2 \sin(2\omega t + \varphi)]$$

where  $A^2$ ,  $B^2$  and  $\varphi$  are functions of the initial conditions only. The maximum value of  $r$ , thus the beam radius, changes in time as  $(\gamma \omega)^{-\frac{1}{2}}$ , or:

$$\frac{r(t)}{r(0)} = \frac{|u(t)|}{|u(0)|} = \left| \frac{\gamma^{-\frac{1}{2}}(t) z(t)}{z(0)} \right| = \left[ \frac{(\Omega_z^2 + 2\Omega_y^2 - 4\Omega^2)_0}{\gamma^2(t) (\Omega_z^2 + 2\Omega_y^2 - 4\Omega^2)_t} \right]^{\frac{1}{4}} \quad (4.5)$$

During inductive charging  $\Omega_y \approx 0$  and  $\gamma \approx 1$ . If  $\Omega \approx 0$  we get the well-known adiabatic condition

$$r^2(t) B_z(t) = \text{const} \quad (4.6)$$

This is equivalent to  $\frac{v_{\perp}^2}{B} = \text{const}$ .

As acceleration takes place  $\Omega_y$  rises and  $\Omega^2$  drops down (like  $\gamma^3$ ). At high  $\gamma$  the self term is always negligible due to cancellation of the electric and magnetic forces. The beam radius then changes as

$$r(t) (B_z^2 + 2B_y^2)^{\frac{1}{4}} = \text{const} \quad (4.7)$$

Thus the beam is further compressed as it is accelerated. If, after  $B_y$  reaches its maximum,  $B_z$  is turned off, the final beam radius will be  $r_f/r_o = (B_{zo}^2/2B_{yf}^2)^{1/4}$ . For  $B_{zo} = 10$  kG,  $B_{yf} = 5$  kG,  $r_f/r_o = 1.2$ .

At a final energy of 300 MeV  $\epsilon/\pi = \frac{\bar{v}}{c} \frac{1.2r_o}{\gamma c} = 2$  millirad cm. Instabilities may increase this number. As the emittance depends mainly on the injection method, a full understanding of this process will be necessary to further increase the beam quality.

The electron ring dynamics during acceleration is very similar to the one electron dynamics. Here, however, the electrostatic interaction with the walls does not reduce during acceleration and according to (4.5) the amplitude increases as:

$$r(t) \left[ 1 + \frac{2B_y^2}{B_z^2} - 2\gamma \left( \frac{r_b}{a} \right)^2 \left( \frac{\omega_o}{\Omega_z} \right)^2 \right]^{1/4} = \text{const} \quad (4.8)$$

For the standard parameters the change in  $r$  is negligible, even for  $\gamma = 600$ . If, however, the line density is increased by an order of magnitude, the beam will become unstable at  $\gamma \approx 200$ . This can be remedied by increasing the toroidal field or by the persisting image currents in the walls (compare to Eq. (3.9)).



## V. FERMI DRIFT

A charged particle moving along a toroidal magnetic field drifts with a constant speed in a direction perpendicular to the toroidal plane. This drift is known as the Fermi (sometimes also  $\bar{v}B$ ) drift. It is due to the non-constancy of the magnetic field (necessary for  $\bar{v} \times \bar{B} = 0$ ) as a function of the radius. This effect is of second order in  $(a/R)$  and was neglected in the previous discussion. In the Betatron we describe, which has both toroidal and vertical magnetic fields, and which has strong self-fields, the Fermi drift motion is weakened as we shall see.

Let us start with the simple case of electron moving along a toroidal fields. The equations of motion in the transverse directions are:

$$\ddot{x} + \hat{\Omega}_z(x) \dot{y} = 0 \quad (5.1)$$

$$\ddot{y} - \hat{\Omega}_z(x) \dot{x} = 0$$

where

$$\hat{\Omega}_z = \frac{\Omega_z R}{(R-x)} \approx \Omega_z \left(1 + \frac{x}{R}\right) \quad (5.2)$$

up to first order in  $(x/R)$ .  $R$  is the radius of the equilibrium Betatron orbit. Equations (5.1) are non-linear. To use perturbation technique let us first write them in the following way:

$$\ddot{x} + \Omega_z \dot{y} \approx - \Omega_z \frac{x}{R} \dot{y} \quad (5.1')$$

$$\ddot{y} - \Omega_z \dot{x} \approx \Omega_z \frac{x}{R} \dot{x}$$

Writing  $x = x^{(1)} + x^{(2)} + \dots$ ,  $y = y^{(1)} + y^{(2)} + \dots$

where

$$\begin{aligned}\ddot{x}^{(1)} + \Omega_z \dot{y}^{(1)} &= 0 \\ \ddot{y}^{(2)} - \Omega_z \dot{x}^{(1)} &= 0\end{aligned}\tag{5.3}$$

with the given initial conditions, and

$$\begin{aligned}\ddot{x}^{(2)} + \Omega_z \dot{y}^{(2)} &= -\Omega_z \frac{(x \cdot \dot{y})^{(2)}}{R} = -\Omega_z \frac{x^{(1)} \dot{y}^{(1)}}{R} \\ \ddot{y}^{(2)} - \Omega_z \dot{x}^{(2)} &= \Omega_z \frac{(x \cdot \dot{x})^{(2)}}{R} = \Omega_z \frac{x^{(1)} \dot{x}^{(1)}}{R}\end{aligned}\tag{5.4}$$

with the initial conditions  $x^{(2)} = y^{(2)} = 0$ ,  $\dot{x}^{(2)} = \dot{y}^{(2)} = 0$ .

Higher order terms will be neglected, consistent with Eq. (5.2).

The solution to Eq. (5.3) can be written without any loss of generality as:

$$\begin{aligned}x^{(1)} &= x_0 \cos \Omega_z t \\ y^{(1)} &= \frac{\dot{y}_0}{\Omega_z} \sin \Omega_z t\end{aligned}\tag{5.5}$$

where

$$\dot{y}_0 = \Omega_z x_0$$

Inserting this into Eq. (5.4) we get the inhomogeneous equations

$$\begin{aligned}\ddot{x}^{(2)} + \Omega_z \dot{y}^{(2)} &= -\Omega_z \frac{x_0 \dot{y}_0}{2R} (1 + \cos 2\Omega_z t) \\ \ddot{y}^{(2)} - \Omega_z \dot{x}^{(2)} &= \Omega_z^2 \frac{x_0^2}{2R} \sin 2\Omega_z t\end{aligned}\tag{5.6}$$

with initial conditions  $x_{(0)}^{(2)} - y_{(0)}^{(2)} = 0$ ,  $\dot{x}_{(0)}^{(2)} - \dot{y}_{(0)}^{(2)} = 0$ .

These equations can be separated;

$$\begin{aligned} \ddot{x}^{(2)} + \Omega_z^2 x^{(2)} = & - \left( \Omega_z \frac{x_0 \dot{y}_0}{2R} + \Omega_z^2 \frac{x_0^2}{4R} \right) \\ & - \left( \Omega_z \frac{x_0 \dot{y}_0}{2R} - \Omega_z^2 \frac{x_0^2}{4R} \right) \cos 2\Omega_z t \end{aligned} \quad (5.7)$$

$$\ddot{y}^{(2)} + \Omega_z^2 y^{(2)} = \left( \Omega_z^2 \frac{x_0^2}{2R} - \frac{x_0 \dot{y}_0}{4R} \right) \sin 2\Omega_z t - \Omega_z^2 \frac{x_0 \dot{y}_0}{2R} \cdot t$$

The solution to the first equation is obtained immediately.

$$x^{(2)} = a(\cos \Omega_z t - 1) + b(\cos 2\Omega_z t - 1) \quad (5.8a)$$

where

$$a + b = \left( \Omega_z \frac{x_0 \dot{y}_0}{2R} + \Omega_z^2 \frac{x_0^2}{4R} \right) / \Omega_z^2$$

and

$$b = \left( \Omega_z \frac{x_0 \dot{y}_0}{2R} - \Omega_z^2 \frac{x_0^2}{4R} \right) / 3\Omega_z^2$$

Thus the second order correction to  $x$  is a sum of two simple oscillations with frequencies  $\Omega_z$  and  $2\Omega_z$ , shifted  $\sim (a+b)$  relative to the first order gyro center. Substituting  $\dot{y}_0 = \Omega_z x_0$ , the shift is

$$|\Delta x| = \frac{3x_0^2}{4R} \ll x_0$$

thus it is negligible.

The solution to the  $y^{(2)}$  equation is also immediate.

$$y^{(2)} = - \left( \frac{x_0^2}{2R} - \frac{x_0 \dot{y}_0}{4R\Omega_z} \right) \sin 2\Omega_z t - \frac{x_0 \dot{y}_0}{2R} t \quad (5.8b)$$

Thus, in addition to the small amplitude oscillation, there appears a drift term with speed

$$\dot{y}_D = - \frac{\gamma m v_{\perp}^2}{2B} \frac{c}{qR} = - \mu \frac{c}{qR} \quad (5.9)$$

where  $\mu$  is the electron magnetic moment.

In conclusion, up to second order we found that the electron rotates around its guiding center which drifts in the  $-y$  direction with constant speed.

Now let us return to the modified Betatron case. For simplicity assume  $s = 1/2$ . The equations of motion up to second order are:

$$\ddot{x} + \Omega_z \dot{y} + \omega^2 x = - \Omega_z \frac{x}{R} \dot{y} \quad (5.10)$$

$$\ddot{y} - \Omega_z \dot{x} + \omega^2 y = \Omega_z \frac{x}{R} \dot{x}$$

where

$$\omega^2 = \frac{1}{2} \Omega_y^2 - \Omega^2 \quad (5.10')$$

The first order solution is given by a combination of the modes:

$$\omega^{\pm} = \frac{\Omega_z \pm \sqrt{\Omega_z^2 + 4\omega^2}}{2} \quad (5.11)$$

The general form of the solution is:

$$\begin{pmatrix} x \\ \dot{x} \\ y \\ \dot{y} \end{pmatrix} = -A \begin{pmatrix} 1 \\ i\omega^+ \\ -i \\ \omega^+ \end{pmatrix} e^{i\omega^+ t} + B \begin{pmatrix} 1 \\ i\omega^- \\ -i \\ \omega^- \end{pmatrix} e^{i\omega^- t} + C \begin{pmatrix} 1 \\ -i\omega^+ \\ i \\ \omega^+ \end{pmatrix} e^{-i\omega^+ t} + D \begin{pmatrix} 1 \\ -i\omega^- \\ i \\ \omega^- \end{pmatrix} e^{-i\omega^- t} \quad (5.12)$$

where the constants A, B, C, D, should be determined by the four initial conditions.

It will be shown that the Fermi drift is important here only when  $\omega \ll \Omega_z$ , thus

$$\begin{aligned} \omega^+ &\approx \Omega_z \\ \omega^- &\approx -\frac{\omega^2}{\Omega_z} \end{aligned} \quad (5.13)$$

The equations for the second order corrections are:

$$\begin{aligned} \ddot{x}^{(2)} + \Omega_z \dot{y}^{(2)} + \omega^2 x^{(2)} &= -\Omega_z \frac{x^{(1)}}{R} \dot{y}^{(1)} \equiv g_x(t) \\ \ddot{y}^{(2)} - \Omega_z \dot{x}^{(2)} + \omega^2 y^{(2)} &= \Omega_z \frac{x^{(1)}}{R} \dot{x}^{(1)} \equiv g_y(t) \end{aligned} \quad (5.14)$$

The solution to these equations can be obtained by using the method called variation of constants.

Given the set of equations

$$\dot{y} = A(t)y + g(t) \quad (5.15)$$

where A is an  $n \times n$  matrix, y,  $\dot{y}$  and g are n-vectors. Assume  $\Phi$  is the fundamental matrix of  $\dot{y} = A(t)y$ . Then the function

$$u(t) = \Phi(t) \int_0^t \Phi^{-1}(s) g(s) ds \quad (5.16)$$

is the unique solution of (5.15) with the initial conditions  $u(0) = 0$ . From (5.12) and (5.16) we obtain this solution:

$$\begin{aligned} x^{(2)} = & \frac{1}{\omega^+ - \omega^-} \left\{ \int_0^t g_x(s) [\sin \omega^+(t-s) - \sin \omega^-(t-s)] ds \right. \\ & \left. + \int_0^t g_y(s) [\cos \omega^+(t-s) - \cos \omega^-(t-s)] ds \right\} \\ y^{(2)} = & \frac{1}{\omega^+ - \omega^-} \left\{ \int_0^t g_x(s) [\cos \omega^-(t-s) - \cos \omega^+(t-s)] ds \right. \\ & \left. + \int_0^t g_y(s) [\sin \omega^+(t-s) - \sin \omega^-(t-s)] ds \right\} \end{aligned} \quad (5.17)$$

The term that gives rise to the Fermi drift in the limit  $\omega^- \rightarrow 0$  is

$$y_D^{(2)} = \frac{1}{\omega^+ - \omega^-} \int_0^t g_x(s) \cos \omega^-(t-s) ds \quad (5.18)$$

The other terms are analogous to the oscillating and the small shifting terms in (5.8). Moreover, it is only the constant part of  $g_x(s)$  which contributes to the Fermi drift. It can be shown by a straightforward calculation that

$$y_D^{(2)} = - \frac{\Omega_z}{2R(\omega^+ - \omega^-)^3} \left[ \Omega_z(\dot{x}_0^2 + \dot{y}_0^2) - \omega^2 \Omega_z(x_0^2 + y_0^2) + 2\omega^2(x_0\dot{y}_0 - y_0\dot{x}_0) \right] \frac{\sin \omega^- t}{\omega^-} \quad (5.19)$$

The dominant term in the sum is  $\Omega_z(\dot{x}_0^2 + \dot{y}_0^2)$ , thus we get

$$y_D^{(2)} \approx - \frac{v_\perp^2}{2R\Omega_z} \cdot \frac{\sin \omega^- t}{\omega^-} \quad (5.20)$$

The Fermi drift speed is multiplied by  $\cos \omega^- t$ , and the electron will drift only a finite distance,  $\Delta y$ , up and down.

$$|\Delta y| = \frac{v_\perp^2}{2R\Omega_z |\omega^-|} \approx \frac{1}{2R} \left| \frac{v_\perp}{\omega} \right|^2 \quad (5.21)$$

If  $|\Delta y| \ll a$  the Fermi drift can be neglected.

Close to injection  $|\omega^2| = \Omega^2 = \frac{\omega_p^2}{2}$  and  $\gamma \approx 1$ , thus the above criterion is

$$\left( \frac{v_\perp}{\omega_p} \right)^2 \ll aR \quad \text{or} \quad \beta_{O_\perp}^2 \ll 2\pi n a R r_c \quad (5.22)$$

where  $n$  is the electron density and  $r_c$  is the electron classical radius. For  $n = 10^{11} \text{ cm}^{-3}$ ,  $\beta_{O_\perp}^2 = 0.5$ ,  $a = 5 \text{ cm}$ ,  $R = 100 \text{ cm}$ , inequality (5.22) is satisfied.

When  $\gamma$  is large  $\frac{1}{2}\Omega_y^2 > \Omega^2$  and the Fermi drift can be still negligible due to the focusing effect of the Betatron field. The condition for this is  $(v_\perp/v_\parallel)^2 \ll a/R$ , but since  $v_\perp = v_\perp^0/\gamma$  it can

be written as:

$$(v_{\perp}^0/v_{\parallel})^2 \ll (a/R) \gamma^2 \quad (5.23)$$

Assuming  $v_{\parallel} \approx c$  and  $(v_{\perp}^0/c)^2 = \frac{1}{2} (5.23)$  yields  $\gamma^2 \gg 10$ .

A problem exists only when  $\frac{1}{2}\Omega_y^2 = \Omega^2$ . This occurs at  $\gamma \approx 13$  (see 2.10). In order to prevent the beam from displacing to the wall a rapid change of  $\gamma$  should take place. However, a simple calculation shows that  $\gamma$  should be changed from  $\sim 12$  to  $\sim 14$  in about 30 nsec which is not practical. It turns out, however, that the surrounding metallic walls help in preventing a catastrophe. In the preceding discussion, we assumed that the beam is located at the center of the torus and neglected interaction with the walls. A displacement of the beam will induce non-negligible electric image forces. The equations of motion for the beam center can be obtained by averaging (5-10) over all the electrons. Let us denote the coordinates of the beam center by  $X, Y$  and the single particle coordinates by  $x, y$ :

$$\ddot{X} + \Omega_z \dot{Y} + \omega_b^2 X = - \frac{\Omega_z}{R} \langle xy \rangle \quad (5.24)$$

$$\ddot{Y} - \Omega_z \dot{X} + \omega_b^2 Y = \frac{\Omega_z}{R} \langle x\dot{x} \rangle$$

where  $\omega_b^2 = \frac{1}{2}\Omega_y^2 - \left(\frac{r_b}{a}\right)^2 \Omega_b^2$ . (5.25)

$r_b$  is the beam radius and  $\Omega_b^2 = \frac{\omega_p^2}{2}$ .

The average terms can be calculated immediately.



$$\langle x\dot{x} \rangle = \langle (X + \delta x) (\dot{X} + \delta\dot{x}) \rangle = X\dot{X} + \frac{1}{2}\langle \delta\dot{x}^2 \rangle = X\dot{X}$$

$\delta x$  is the x coordinate of a single electron relative to the beam center.  $\langle \delta\dot{x}^2 \rangle = 0$  because the beam x-dimension does not change as it drifts.

$$\langle x\dot{y} \rangle = X\dot{Y} + \langle \delta x \cdot \delta\dot{y} \rangle = X\dot{Y} + \frac{\langle v_{\perp}^2 \rangle}{2\Omega_z}$$

where  $\langle \delta x \cdot \delta\dot{y} \rangle$  was estimated exactly as (5.20). The equations of motion of the beam center are:

$$\begin{aligned} \ddot{X} + \Omega_z \dot{Y} + \omega_b^2 X &= -\frac{\Omega_z}{R} X \dot{Y} - \frac{\langle v_{\perp}^2 \rangle}{2R} \\ \ddot{Y} - \Omega_z \dot{X} + \omega_b^2 Y &= X \dot{X} \end{aligned} \tag{5.26}$$

The constant term on the r.h.s. result in a small shifting of the beam in the -x direction (outside) unless  $\omega_b^2 = 0$ . If  $\omega_b = 0$  a drift in the y direction with a speed  $\frac{-\langle v_{\perp}^2 \rangle}{2R\Omega_z}$  will start.

In comparing (5.26) to (5.10) it is evident that the beam and the single particle drifts occur at different  $\gamma$  (compare equations 3.10) and 2.10). Thus when the single particle drift starts the beam is stable and it will only oscillate with a small amplitude. In order to estimate this single particle drift effect assume that at  $t=0$  the beam is located at  $X=Y=0$ , and it starts

drifting with  $\dot{x}_0 = 0$ ,  $\dot{y}_0 = -\frac{\langle v_{\perp}^2 \rangle}{2R\Omega_z}$ . Following the same steps as for the single particle case, we find that the beam will oscillate in the y direction with amplitude:

$$|\Delta y| = \frac{\dot{y}_0^2}{2R\Omega_z |\omega^-|} \quad \text{where} \quad |\omega^-| = \left| \frac{\omega_b^2}{\Omega_z} \right|$$

or

$$|\Delta y| = \frac{1}{2R} \left| \frac{\dot{y}_0}{\omega_b} \right|^2$$

Thus, the criterion for the single particle Fermi drift to be negligible is

$$\left| \frac{\dot{y}_0}{\omega_b} \right| \ll \sqrt{2Ra} \quad (5.27)$$

$\omega_b$  can be estimated if we assume that at the transition  $\frac{1}{2}\Omega_y^2 \ll (r_b/a)^2 \Omega_b^2$ , then we get

$$\langle \beta_{o_{\perp}}^2 \rangle \ll \frac{2\Omega_z^0 \omega_p^0}{c^2} \left( \frac{r_b}{a} \right) \sqrt{Ra} R \quad (5.28)$$

In our standard example, this inequality is obviously satisfied.

As  $\gamma$  increases further, the beam will become unstable for  $\omega_b = 0$  and will quickly drift to the wall (see Section 3 for other instabilities which occur at this region).

## VI. RESONANCE INSTABILITIES

In the previous discussion we assumed that all the fields were ideal, i.e., they did not depend upon the coordinate  $z$ . Errors in these fields give rise to new types of phenomena, known as orbital resonances or parametric instabilities. These instabilities might very easily destroy the beam quality, and it is our purpose here to give quantitative restrictions on the fields in order to assure good beam quality. We shall treat the equations of motion only in the linear approximation. Higher orders are important only when the beam quality is so poor that they are of no interest anyway.

In the previous discussion, the fields were expanded around the equilibrium radius,  $R$ , and the expansion parameters were assumed constant. Now we let them be functions of  $z$ . If the electrons move with constant  $v_z$ , these parameters are also periodic functions of time, with a period  $T$ , ( $T = \frac{2\pi R}{v_z}$ ). When  $T$  is an integral (sometimes half integral) multiple of the transverse oscillation time, a resonance occurs. We shall examine some of the interesting cases and find the restrictions they impose on the external fields.

We shall start with perturbing the Betatron field  $B_y$ . This necessarily perturbs the equilibrium radius  $R$ . Electrons will be deflected in the  $x$  direction. In certain conditions they will resonate with the  $\delta B_y(z)$  field. We shall derive these conditions and determine their influence on the operation of the high current Betatron.  $\delta B_y(z)$  induces additional component  $\delta B_z(y)$  ( $\vec{\nabla} \times \vec{B} = 0$ ).

This will, however, add only second order terms to the equations of motion and thus will be neglected.

Assuming  $\delta B_x = 0$ , the Betatron field will be

$$B_y \approx B_0 \left(1 + \frac{sx}{R}\right) + \delta B_y(z) \quad (6.1)$$

$$B_x \approx B_0 \frac{sx}{R}$$

and the equations of motion.

$$\ddot{x} + \frac{\dot{Y}}{Y} \dot{x} + \Omega_z \dot{y} + \left[(1-s)\Omega_y^2 - \Omega^2\right] x = \Omega_y^2 R \frac{\delta B_y(z)}{B_0} \quad (6.2)$$

$$\ddot{y} + \frac{\dot{Y}}{Y} \dot{y} - \Omega_z \dot{x} + \left[s\Omega_y^2 - \Omega^2\right] y = 0$$

In discussing (6.2) let us start with the conventional Betatron, i.e., without toroidal field. We shall see later that the high current Betatron can be analyzed by a simple generalization. The equation of motion for the x component is:

$$\ddot{x} + \frac{\dot{Y}}{Y} \dot{x} + \omega^2 x = \Omega_0^2 R \epsilon(t) \quad (6.3)$$

where  $\Omega_0 = \Omega_y = \frac{v_z}{R} \approx \frac{c}{R}$ ,  $\omega^2 = \frac{1}{2}\Omega_y^2 - \Omega^2$  and it changes slowly in time.  $\epsilon(t)$  is periodic in  $t$  with period  $T = \frac{2\pi}{\Omega_0}$ , and thus can be decomposed in a Fourier series:

$$\epsilon(t) = \sum_{n=1}^{\infty} (\alpha_n \cos n \Omega_0 t + \beta_n \sin n \Omega_0 t)$$

$$\alpha_n = \frac{2}{T} \int_0^T \epsilon(t) \cos n \Omega_0 t dt \quad (6.4)$$

$$\beta_n = \frac{2}{T} \int_0^T \epsilon(t) \sin n \Omega_0 t dt$$

If  $\omega$  and  $\gamma$  are constant the solution to (6.3) with the given initial conditions is:

$$x = x_0 \cos \omega t + \frac{\dot{x}_0}{\omega} \sin \omega t + \frac{1}{\omega} \int_0^t \Omega_0^2 R \epsilon(s) \sin \omega(t-s) ds \quad (6.5)$$

Substituting (6.4) for  $\epsilon(s)$ , the integral can be calculated explicitly. A special case is for  $\omega = n \Omega_0$ . Then we find for the integral  $\frac{\Omega_0 R}{2n} [\alpha_n \sin n \Omega_0 t - \beta_n \cos n \Omega_0 t] t + \sum_{k \neq n} (\text{non secular terms})$ .

Thus the amplitude grows linearly with time.

A conventional Betatron operates below the  $n=1$  resonance. In the modified Betatron, we start with very large  $n$  and go down to the lowest resonances as  $\gamma$  increases. It is thus necessary to estimate the amplitude growth as resonances are crossed.

For large  $n$  resonances are crossed so quickly that no growth (or at least a very small growth) in the amplitude is expected. When the time  $\Delta t_n$ , to go from  $\omega = (n + \frac{1}{2}) \Omega_0$  to  $\omega = (n - \frac{1}{2}) \Omega_0$  is comparable to  $T$ , the time to go around the torus, a real growth in the amplitude might occur.  $\Delta t_n$  is given by:

$$\left| \frac{\partial \omega}{\partial t} \right|_{\omega = n \Omega_0} \cdot \Delta t_n = \Omega_0 \quad (6.6)$$

Take, for simplicity, only the  $\cos n \Omega_0 t$  term of the Fourier series and denote

$$\delta\omega = \omega - n \Omega_0$$

$$\bar{\omega} = (\omega + n \Omega_0)/2$$

then the resonant term will be

$$X_{\text{res}} = \frac{\Omega_0^2 R \alpha_n}{2\bar{\omega}} \cdot \frac{\sin \delta\omega t}{\delta\omega} \sin \bar{\omega} t \quad (6.7)$$

Thus, the amplitude for  $\delta\omega \neq 0$  goes like  $(\delta\omega)^{-1}$ . This is the reason that real growth occurs only very close to resonance, and each resonance can be taken separately. Thus, let us look only on the  $n$  resonance as it is crossed.

If  $\frac{1}{\omega^2} \frac{\partial\omega}{\partial t} \ll 1$ , the asymptotic expansion WKB can be employed. It can be shown then that the solution to (6.3) is:

$$X = \frac{x_0}{\sqrt{\gamma\omega}} \cos \omega t + \frac{\dot{x}_0}{\gamma\omega} \sin \omega t + \Omega_0^2 R \int_0^t \frac{\epsilon(s)}{\omega(s)} \sin [\varphi(t) - \varphi(s)] ds$$

where

$$\varphi(t) = \int_0^t \omega(t') dt' \quad (6.8)$$

In the high current Betatron  $\gamma\omega$  is nearly constant, thus the zero order amplitude is constant, while the transverse speed decreases as  $\gamma^{-1}$ . The integral may, however, increase the amplitude due to the resonance terms, which can be shown to be

$$X_{\text{res}} = \frac{\Omega_0^2 R \alpha_n}{2} \left[ \int_0^t \frac{\cos [\varphi(s) - n \Omega_0 s]}{\omega(s)} ds \right] \sin \varphi(t) \quad (6.9)$$

The last integral can be approximated by:

$$\begin{aligned} \frac{1}{\bar{\omega}} \int_{-\frac{\Delta t_n}{2}}^{\frac{\Delta t_n}{2}} \cos \left[ \frac{1}{2} \left( \frac{\partial \omega}{\partial t} \right)_{\omega=n\Omega_0} \cdot s^2 \right] ds &= \frac{2\sqrt{2}}{\bar{\omega} \sqrt{\frac{\partial \omega}{\partial t}}} \int_0^{\frac{\sqrt{2}(\frac{\partial \omega}{\partial t}) \frac{\Delta t_n}{2}}{2}} \cos t^2 dt \\ &= \frac{2}{\sqrt{\pi}} \frac{T \sqrt{N_n}}{\bar{\omega}} \int_0^{\sqrt{\frac{\pi}{2}} N_n} \cos t^2 dt \end{aligned} \quad (6.10)$$

where  $N_n$  is the number of turns the electron does when it goes from  $t=0$  to  $t=\Delta t_n$ . We assumed that  $N_n > 1$ . To estimate the integral (6.10) we note that the function  $\cos t^2$  is close to 1 for  $t < 1$  and is highly oscillating for  $t > 1$ . Thus only the interval  $0 \leq t \leq 1$  contributes significantly to it. Taking  $\bar{\omega} = n \Omega_0$ , the integral (6.10) is estimated to be  $\frac{4\pi}{\sqrt{\pi}} \frac{\sqrt{N_n}}{n \Omega_0^2}$  and substituting back in (6.9) we get the change in the amplitude as we cross the  $n$  resonance:

$$\Delta X_{\text{res}} = \frac{2\pi}{\sqrt{\pi}} \frac{R \alpha_n}{n} \sqrt{N_n} \quad (6.11)$$

To be specific assume that the error is constant ( $\Delta B$ ) in an arc  $L$ , then:

$$\Delta X_{\text{res}} = \left( \frac{\Delta B}{\Delta} \right) \cdot L \cdot \frac{\sqrt{N_n}}{n} \quad (6.12)$$

To minimize  $\Delta X_{res}$ ,  $\Delta B \cdot L$  has to be smaller,  $n$  larger and the time to cross the resonance smaller.

Now let us return to the modified Betatron case in details;

The equations of motion are:

$$\begin{aligned} \ddot{x} + \frac{\dot{\gamma}}{\gamma} \dot{x} + \Omega_z \dot{y} + \omega^2 x &= \Omega_0^2 R \epsilon(t) \\ \ddot{y} + \frac{\dot{\gamma}}{\gamma} \dot{y} - \Omega_z \dot{x} + \omega^2 y &= 0 \end{aligned} \quad (6.13)$$

The change of the solution due to the inhomogeneous term is given by the integrals:

$$\begin{aligned} x(t) &= \frac{\Omega_0^2 R}{(\omega^+ - \omega^-)} \int_0^t \epsilon(s) [\sin \omega^+(t-s) - \sin \omega^-(t-s)] ds \\ y(t) &= \frac{\Omega_0^2 R}{(\omega^+ - \omega^-)} \int_0^t \epsilon(s) [\cos \omega^-(t-s) - \cos \omega^+(t-s)] ds, \end{aligned} \quad (6.14)$$

where  $\omega^\pm$  are given by Eq. 5.11. Resonances occur for  $\omega^\pm = m\Omega_0$ .

However,  $|\omega^-| \approx \frac{\Omega_0^2}{2\Omega_z} < \Omega_0$ , thus only  $\omega^+$  resonances have to be considered and especially the low  $n$  resonances.

Assuming  $\omega_{(0)}^+ \approx 2 \cdot 10^{11} \text{ sec}^{-1}$  ( $B_z^{(0)} = 10^4 \text{ Gauss}$ ), and  $d\gamma/dt \approx 10^6 \text{ sec}^{-1}$ , we obtain

$$\frac{1}{\omega^2} \left| \frac{d\omega}{dt} \right| \approx \frac{1}{\omega\gamma} \left| \frac{d\gamma}{dt} \right| \approx 5 \cdot 10^{-6} \ll 1 \quad (6.15)$$

and WKB can be employed. The results of the one dimensional case are still valid except for an additional factor  $\sim (\Omega_0/\omega^+)^2$ . Moreover, the resonance is now observed also in the  $y$  direction. In our



standard case  $(\Omega_o/\omega^+)^2 \ll 1$ , almost down to the lowest resonance, thus reducing the growth rates predicted earlier. For example, if  $n=2$ ,  $\gamma \approx 340$ ,  $B_y \approx 5$  KGauss and  $(\Omega_o/\omega^+)^2 \approx 0.25$ .

To be specific, let us assume that  $\Delta B_o$  is constant in an arc L, then:

$$\Delta X_{\text{res}}^{(n)} \approx \left(\frac{\Delta B_o}{B_o}\right) L \left(\frac{\Omega_o}{\omega^+}\right)^2 \frac{\sqrt{N_n}}{n}$$

But

$$N_n = \frac{\Omega_o}{\omega_n^+ T \frac{1}{\gamma_n} \left(\frac{dY}{dt}\right)_n}$$

Thus we get the total growth in the amplitude:

$$\Delta X_{\text{res}} = \left(\frac{\Delta B_o}{B_o}\right) L \left(\Omega_o^o / 2\pi \frac{dY}{dt}\right)^{\frac{1}{2}} \sum 1/n^4 \quad (6.16)$$

If  $dY/dt \approx 10^6 \text{ sec}^{-1}$  and  $\Omega_o^o = 2 \cdot 10^{11} \text{ sec}^{-1}$ ,  $\Delta X_{\text{res}} \approx 150 \left(\frac{\Delta B_o}{B_o}\right) L$ . Most of this comes from the  $n=1$  resonance which takes a very long time to cross. Thus it will be useful either to cross the lowest resonances very fast (by turning off  $B_z$  in  $t \approx 10 \mu\text{sec}$ ) or to extract the beam while  $n > 1$ . (e.g., by using the drift motion of the beam - see Sections III and V).

Before discussing the general case let us work out another simple case. Assume that  $B_z$  is perturbed along the torus. According to  $\bar{\nabla} \cdot \bar{B} = 0$ ,  $\frac{\partial}{\partial x} \delta B_x + \frac{\partial}{\partial y} \delta B_y \neq 0$  and additional first order terms should be included in the equations of motion. If  $\frac{\partial}{\partial x} \delta B_x = \frac{\partial}{\partial y} \delta B_y$  and if  $\delta B_x(o,o) = \delta B_y(o,o) = 0$  the equations of

motion are:

$$\begin{aligned} \ddot{x} + \frac{\dot{\gamma}}{\gamma} \dot{x} + \Omega_z \dot{y} + \frac{1}{2} \dot{\Omega}_z y + \left[ \frac{1}{2} \Omega_y^2 - \Omega^2 \right] x &= 0 \\ \ddot{y} + \frac{\dot{\gamma}}{\gamma} \dot{y} - \Omega_z \dot{x} - \frac{1}{2} \dot{\Omega}_z x + \left[ \frac{1}{2} \Omega_y^2 - \Omega^2 \right] y &= 0 \end{aligned} \quad (6.17)$$

Neglecting the terms with  $\dot{\gamma}/\gamma$  and using the transformation

$$x + iy = \exp \left[ i/2 \int_0^t \Omega_z(t') dt' \right] u(t) \quad (6.18)$$

we get

$$\ddot{u} + \omega^2(z) u = 0 \quad (6.19)$$

where

$$\omega = \frac{1}{2} \sqrt{\Omega_z^2 + 2\Omega_y^2 - 4\Omega^2}$$

When  $\omega$  is constant the general solution is:

$$u = A \cos \omega t + B \sin \omega t = u_x + i u_y \quad (6.20)$$

and  $u_x = \operatorname{Re} u$ ,  $u_y = \operatorname{Im} u$ . The four initial conditions are:

$$\begin{aligned} u_x(0) = x(0) & \quad ; \quad u_y(0) = y(0) \\ \dot{u}_x(0) = \dot{x}(0) + \frac{\Omega_z}{2} y(0) & \quad ; \quad \dot{u}_y(0) = \dot{y}(0) - \frac{\Omega_z}{2} x(0) \end{aligned} \quad (6.21)$$

Unlike Eqs. (6.17), (6.19) for  $u_x$  and  $u_y$  are not coupled, even when  $\omega$  is not constant.

For the stability analysis it is enough to examine  $|u| = |x + iy|$ . The amplitude growth rate is determined by the

two real equations

$$\ddot{u}_i + \omega^2(z) u_i = 0$$

where

$$i = x, y .$$

The two independent solutions to each of these equations can be written according to Floquet's theorem as:

$$u(t) = e^{i\mu t} g_\mu(t) \quad (6.22)$$

where  $g_\mu(t+T) = g_\mu(t)$  and the constant  $\mu$  is either real or pure imaginary. For  $\omega$  constant it is readily verified that  $\mu = \pm \omega_0$ . However, when a small perturbation is added to  $\omega_0$ , there will be regions of  $\omega_0$  for which  $\mu$  will become pure imaginary and one of the two independent solutions will be unstable.

To show this explicitly let us take the following example, which can be solved analytically:

Assume

$$\omega(t) = \begin{cases} \omega_0(1+Q) & 0 < t < a = T/M \\ \omega_0 & a < t < T \end{cases} \quad (6.23)$$

$b = T - a$ , and  $\omega(t+T) = \omega(t)$ . It can be shown that:

$$\cos \mu T = \cos[\omega_0(T+aQ)] - \frac{Q^2}{2(1+Q)} \sin[\omega_0 a(1+Q)] \sin(\omega_0 b) \quad (6.24)$$

As  $Q \rightarrow 0$  the r.h.s. becomes  $\cos \omega_0 T$ . Resonances are expected around  $\omega_0 T = n\pi$ . If  $Q \neq 0$  the r.h.s. might be greater than 1 (in absolute value) in some intervals. For these intervals  $\mu$

will be imaginary and the orbital amplitude will grow indefinitely in time.

In order to find the locations and widths of these intervals define

$$X = \omega_0 [T + aQ] \quad (6.25)$$

The r.h.s. of Eq. (6.24) can be written as:

$$(\text{r.h.s.}) = \cos X (1 + G \sin^2 \omega_0 b) - \frac{G}{2} \sin 2\omega_0 b \sin X \quad (6.26)$$

where

$$G = \frac{Q^2}{2(1+Q)}$$

If  $|G| \ll 1$  the r.h.s. can be  $\pm 1$  only when  $\cos X \approx \pm 1$  or  $X \approx n\pi$ , or

$$\omega_0^{(n)} = \frac{\frac{n}{2} \Omega_0}{(1 + Q a/T)} \quad (6.27)$$

Expanding the r.h.s. around  $\omega_0 = \omega_0^{(n)}$  we get:

$$\text{r.h.s.} = (-)^n [1 + G \sin^2 \omega_0^{(n)} b] - \frac{G}{2} \sin 2\omega_0^{(n)} b (\delta X) - \frac{1}{2} (\delta X)^2 \quad (6.28)$$

The maximum of this expression is obtained at

$$\delta X = - \frac{G}{2} \sin 2\omega_0^{(n)} b$$

and is  $1 + G \sin^2 \omega_0^{(n)} b$  to first order in  $G$ . The width of the  $n$  unstable region is

$$\delta \omega_0^{(n)} = \frac{\sqrt{8G}}{T} |\sin \omega_0^{(n)} b| = \frac{2Q}{T} |\sin \omega_0^{(n)} b| \quad (6.29)$$

For small  $n$  resonances ( $n \ll M$ )

$$\delta \omega_o^{(n)} \approx Q \frac{n}{M} \Omega_o \quad (6.30)$$

and the e-folding time,  $t_n$ , at the maximum growth rate is

$$t_n \approx \frac{1}{\pi Q} \cdot \frac{M}{n} \cdot T \quad (6.31)$$

In the high current Betatron  $\omega_o$  changes in time, due to the change in  $\gamma$  or  $B_z$ . At the beginning  $B_z$  is held constant ( $\sim 10$  kG) and  $\gamma$  rises. In our standard example  $n\gamma \approx 670$  and unless  $\gamma$  is very high  $n \gg 1$ . For  $n \geq M$  the number of turns that an electron executes while it crosses the  $n$ -th resonance is  $\leq 10^4 \frac{Q}{n^2}$ . Thus until  $n$  is very low this number is much smaller than 1 and no real growth is expected. As  $n$  becomes of the order of 1 ( $n \ll M$ ) the number of turns the electron stays in the  $n$ -th resonance is  $\sim 3 \cdot 10^4 \frac{Q}{nM}$ . Assuming  $Q = 10^{-2}$ ,  $M = 10$ , and  $n = 1$  this number is  $\sim 30$ . The amplitude growth will be less than 10%. Comparing to Eq. (6.16) it is obvious that the same perturbation in  $\delta B_y$  is much more destructive.

As we pointed out earlier the missing of the half integral resonances in the last case was due to the high symmetry of the problem. In order to see the general nature of the motion as  $B_z$  is perturbed assume that  $\partial \delta B_x / \partial x = 0$ . Thus  $\partial \delta B_y / \partial y = - \partial \delta B_z / \partial z$  and the equations of motion become

$$\ddot{x} + (\Omega_z' y) = 0 \quad (6.32)$$

$$\ddot{y} - \Omega_z' x = 0$$

Integrating the first equation and substituting in the second we get

$$\begin{aligned}\dot{x} + \Omega_z y &= \dot{x}^{(0)} + (\Omega_z y)^{(0)} = A \\ \ddot{y} + \Omega_z^2 y &= A \Omega_z = A(\hat{\Omega}_z + \delta\Omega_z)\end{aligned}\tag{6.33}$$

where  $\hat{\Omega}_z$  is the average along the torus and A is a constant which depends upon the initial conditions. The second equation is a nonhomogeneous Hill's equation and it has integral and half integral resonances. The symmetry in this case is obviously lower than in the previous case.

Let us now consider the most general perturbations in the fields for a high current Betatron. These fields may be expanded around the average equilibrium radius  $R = v_z/\Omega_0$ . Using Maxwell's equations  $\bar{\nabla} \cdot \bar{B} = 0$ ,  $\bar{\nabla} \times \bar{B} = 0$  and keeping terms only up to first order in the equations of motion we get:

$$\begin{aligned}\ddot{x} + \frac{\dot{y}}{y} \dot{x} + \Omega_z \dot{y} + \left(\frac{1}{2} \Omega_y^2 - \Omega^2\right) x &= \Omega_y^2 R \frac{\delta B_0}{B_0} + \Omega_y^2 \left(\frac{\delta B_0}{2B_0} + \delta s\right) x \\ - \Omega_z \left[\frac{\delta B_z}{B_z} \dot{y} + (1 - \alpha) \frac{\delta \dot{B}_z}{B_z} y\right] &\equiv f(t)\end{aligned}$$

$$\ddot{y} + \frac{\dot{y}}{y} \dot{y} - \Omega_z \dot{x} + \left( \frac{1}{2} \Omega_y^2 - \Omega^2 \right) y = - \Omega_y^2 R \frac{\delta B_x}{B_0} - \Omega_y^2 \left( \frac{\delta B_0}{2B_0} + \delta s \right) y$$

$$+ \Omega_z \left[ \frac{\delta B_z}{B_z} \dot{x} + \alpha \frac{\delta \dot{B}_z}{B_z} x \right] \equiv g(t) \quad (6.34)$$

where we assumed  $s = 1/2$  and:

$$B_z = \hat{B}_z + \delta B_z(z)$$

$$B_y = B_0 \left( 1 + \frac{sx}{R} \right) + \delta B_0(z) + \left( \frac{\delta B_0(z)}{B_0} + \frac{\delta s(z)}{s} \right) B_0 \frac{sx}{R} + (\alpha(z) - 1) \frac{\partial \delta B_z}{\partial z} y \quad (6.35)$$

$$B_x = B_0 \frac{sy}{R} + \delta B_x(z) + \left( \frac{\delta B_0}{B_0} + \frac{\delta s}{s} \right) B_0 \frac{sy}{R} - \alpha(z) \frac{\partial \delta B_z}{\partial z} x .$$

$\alpha(z)$  is defined by:

$$\frac{\partial \delta B_x}{\partial x} = - \alpha(z) \frac{\partial \delta B_z}{\partial z} .$$

We wrote the equations of motion so that all the perturbation terms appear on the r.h.s. These terms are, however, not of the same order. The dominant terms are the first, thus one suspects them to be the most dangerous for the beam quality. If  $\delta B_0/B_0$  and  $\delta B_x/B_x$  are given, their contribution can be calculated according to Eq. (5.17).

The first terms result in resonances for  $\omega^+ = n\Omega_0$  ( $\Omega_z > \Omega_y$ ). These resonances were considered in detail (see Eqs. (6.1) - (6.16)). The only difference is that here  $B_x(z)$  is perturbed too.

The growth rate at the resonance is determined mainly by the larger of  $\delta B_x$  and  $\delta B_y$ . Thus to minimize the effect both  $\delta B_x$  and  $\delta B_y$  should be decreased.

The second largest terms on the r.h.s. of Eqs. (6.34) for  $\Omega_z > \Omega_y$  are the  $\Omega_z$  terms. We have seen earlier (see Eqs. (6.17) - (6.31)) that for  $\alpha = 1/2$  these terms give rise to parametric instabilities with  $\sqrt{\Omega_z^2 + 2\Omega_y^2 - 4\Omega^2} = n\Omega_0$ . For  $\alpha \neq 1/2$  new resonances appear ( $|\omega^\pm| = 1/2 n\Omega_0$ ,  $\Omega_z = n\Omega_0$ ). These new modes disappear as  $\alpha \rightarrow 1/2$ . As  $\omega^- \rightarrow 0$  and  $\omega^+ \rightarrow \Omega_z$  (only  $B_z$  is left) we recover the  $\Omega_z = \frac{n}{2} \Omega_0$  resonances (see Eqs. (6.32), (6.33)).

The other terms (proportional to  $\delta B_0/2B_0 + \delta s$ ) give rise to resonances at  $\omega = n\Omega_0$ .

All the instabilities we have just considered start growing linearly. Comparing the terms of the r.h.s. of Eqs. (6.34) it is obvious that the first terms are greater by  $\sim R/r_b$  than the second. This makes the first terms much more destructive. The remaining  $\Omega_z$  terms were investigated carefully and it was found that they are at least one order of magnitude less dangerous than the first terms.



## DISCUSSION

In this paper we investigated some aspects of the stability of a High Current Betatron. Specifically, we discussed (1) space charge limits of both single particle and the electron ring, (2) the Fermi drift, (3) resonance instabilities and (4) beam emittance.

Two important questions have not been addressed, namely; (i) stability during initial acceleration (injection, trapping and initiating acceleration will be discussed separately), (ii) collective modes, such as negative mass and resistive walls. These modes have been discussed extensively by many authors, yet there is no conclusive evidence that they might cause a destructive damage to the High Current Betatron.

Let us summarize the main results:

(1) The space charge limit during injection is increased compared to a conventional Betatron by  $(B_z^2/2B_y^2)$ .

(2) Single particle orbits become unstable (for  $s \neq 1/2$ ) at  $\gamma^3 \approx 4NR^2 r_c / r_b^2$ . This instability, however, is self-stabilized resulting in only a small increase of the beam radius.

(3) The stability of the beam is influenced by the surrounding walls. Ideal conducting walls enhance the stability of the beam relative to the single particle. In the opposite case, when the image currents decay instantaneously the beam may become unstable due to space charge limit as  $\gamma$  increases, even for the  $s = 1/2$  case. This occurs only if the line density is high enough.

(4) For  $s \neq 1/2$  the ring becomes unstable at  $\gamma \approx 4N(R/a)^2 r_c$

(see Eq. (3.10)). In this region the total focusing force on the beam becomes zero and various phenomena occur which make it practically impossible to hold the beam in the torus.

(5) The Fermi drift is negligible except in the region where the total focusing forces on the beam become zero (this is true even for  $s = 1/2$ ). Then, the beam drifts quickly to the wall. This drift may be utilized to extract the beam.

(6) The beam emittance changes only slightly during acceleration (neglecting instabilities). It is, thus, determined by the injection method and by the instabilities enhancement.

(7) Errors in the external fields may cause driven as well as parametric resonances. The first are caused by errors in  $B_y(z)$  or  $B_x(z)$  which are not zero at the equilibrium orbit (monopole-like). These are the most dangerous resonances and put severe restrictions on those fields unless the beam is extracted before they develop ( $n > 1$ ). Parametric resonances (dipole-like), caused by errors in  $B_z(z)$ ,  $B_0(z)$  or  $s(z)$  are much less destructive.

#### Acknowledgements

The authors wish to thank Dr. A. Fisher for stimulating discussions and to Dr. D. Kerst for illuminating some important points during the course of this work.

References

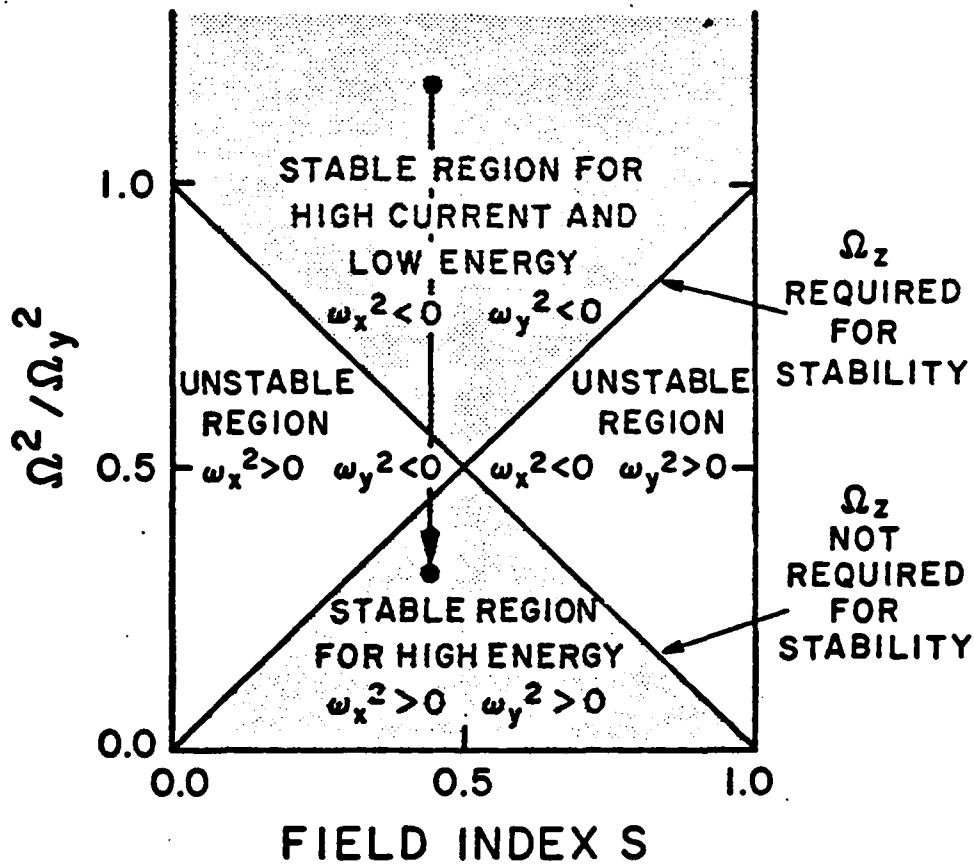
1. D. W. Kerst, G. D. Adams, H. W. Koch, and C. J. Robinson, Phys. Rev. 78, 297 (1950).
2. G. I. Budker, CERN Symposium 1, 68 (1956); 1, 76 (1956).
3. K. C. Rogers, D. Finkelstein, L. Ferrari, D. Caufield, L. Mansfield, and G. Brucker, Proc. Int. Conf. on Accel. CERN, Geneva (1959); P. Reynolds and H. M. Skarsgard, J. Nucl. Energy C1, 36 (1960).
4. I. M. Somoilov and A. A. Sokolov, Soviet Phys. JETP 12, 185 (1961); R. W. Landau and V. K. Neil, Phys. Fluids 12, 2412 (1966).
5. A. I. Pavlevskii, G. D. Kuleshov, G. V. Sklizkov, Y. A. Zysin, and A. I. Gerasimov, Soviet Phys. Doklady 10, 30 (1965); Soviet Phys., Tech. Phys. 22, 210 (1977).
6. N. Rostoker, Comments on Plasma Physics 6, 91 (1980).
7. C. A. Kapetanacos, P. Sprangle, and S. J. Marsh, Bull. Am. Phys. Soc. 26(7), 1047 (1981).
8. A. Fisher, P. Gilad, F. Goldin, and N. Rostoker, Appl. Phys. Lett. 36, 264 (1980), 531 (1980); S. Eckhouse, A. Fisher, and N. Rostoker, Phys. Fluids 21, 1840 (1978).
9. J. D. Daugherty, J. Eninger, and G. S. James, Avco Everett Research Report 375, October 1971.
10. W. Clerk, P. Korn, A. Mondelli, and N. Rostoker, Phys. Rev. Lett. 37, 592 (1976).
11. N. Rostoker, Particle Accelerators 5, 93 (1973).
12. P. Sprangle and C. A. Kapetanacos, J. Appl. Phys. 49, 1 (1978).
13. P. Sprangle, Bull. Am. Phys. Soc. 26(7), 1047 (1981).

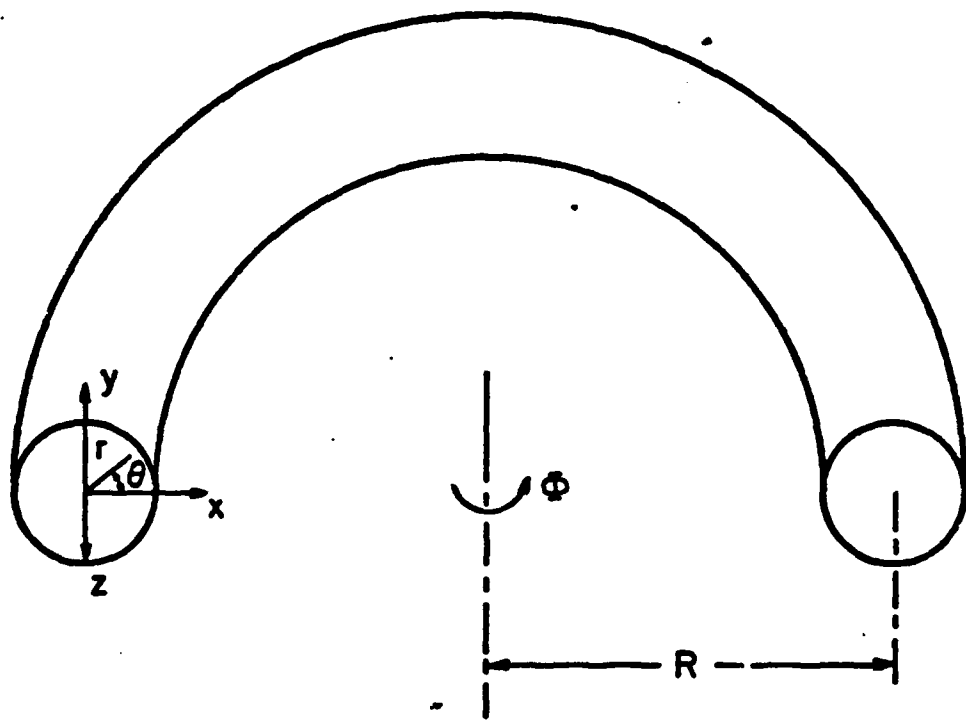
TABLE I: Standard set of parameters for the high current Betatron (used throughout this paper).

Major radius (R)	100	cm
Minor radius (a)	5	cm
$B_z^0$	10	KGauss
Line density (N)	$2 \cdot 10^{11}$	$\text{cm}^{-1}$
Beam radius ( $r_b$ )	1	cm
$\Omega_z^0$	$2 \cdot 10^{11}$	$\text{sec}^{-1}$
$\omega_p^0$	$1.4 \cdot 10^{10}$	$\text{sec}^{-1}$
$B_0/\beta\gamma$	16	Gauss
$d\gamma/dt$	1	$\mu\text{sec}^{-1}$

Figure Captions

- Fig. 1. Schematic design of High Current Betatron with inductive charging.
- Fig. 2. Coordinates for a toroidal electron beam.
- Fig. 3. Graphical representation of the stability conditions for the modified Betatron (see Eq. 2.8)).  
The transition takes place when  $\gamma$  is increased.





UNID

FILMED